1 2 9 0

FACULDADE DE CIÊNCIAS E TECNOLOGIA
UNIVERSIDADE D COIMBRA

Thermal modelling and development of an active water-cooled fireproof barrier

Submitted in Partial Fulfilment of the Requirements for the Degree of Master in Mechanical Engineering in the speciality of Energy and Environment.

Modelação térmica e desenvolvimento de uma barreira antifogo ativa e refrigerada a água

Author

André Filipe Costa Albino

Advisors

Professor Doutor Carlos Xavier Pais Viegas
Professor Doutor Domingos Xavier Filomeno Carlos Viegas

Jury

President	**Professor Doutor António Manuel Gameiro Lopes** **Professor Auxiliar da Universidade de Coimbra**
Vowels	**Professor Doutor Miguel Rosa Oliveira Panão** **Professor Auxiliar da Universidade de Coimbra**
Advisor	**Professor Doutor Carlos Xavier Pais Viegas** **Professor Auxiliar da Universidade de Coimbra**

Institutional Collaboration

INSTITUTE OF SYSTEMS AND ROBOTICS
UNIVERSITY OF COIMBRA

Coimbra, September, 2019

Acredite em si próprio e chegará um dia em que os outros não terão outra escolha senão acreditar com você.

Cynthia Kersey

Aos meus pais.

ACKNOWLEDGEMENTS

The present thesis was not possible to be written without the constant help, guidance and support kindly received from a group of persons which I am profoundly grateful.

My first word goes to my parents and family. During my academic period, their support, comprehension and affection were vital for me, trying always as possible to provide me with the best conditions and resources in order to conclude my academic course.

Beyond my family, I cannot forget the constant affection and patience of my girlfriend Diana. All the motivation and the constant support given were essential to me to keep going and be able to, despite all the adversities, accomplish my personal goals

To my advisor, Prof. Dr Carlos Xavier Pais Viegas, thank you for the incessant help and guidance. The permanent availability to answer my questions and doubts were vital to elaborate the present investigation. To my co-advisor Prof. Dr Domingos Xavier Filomeno Carlos Viegas, a word of gratitude for the scientific knowledge shared as well as the opportunity to elaborate a master thesis regarding such actual issue as wildfires. Without help from Mr Miranda, it would not be possible to use a 3D software used to develop and simulate the steel structure used in the experimental tests. For this reason, I am truly thankful to him. To Prof. Miguel Panão, I would like to express my gratefulness for the theoretical approach guidance as well as the advice given in order to make the best experimental measures as possible.

To CEIF/ADAI team (especially Gonçalo Rosa, Luís Reis, Nuno Luís, Daniela Alves e Cláudia Pinto) thank you for your constant help and knowledge with the experimental tests. Since all of you contributed to the final results reached in this investigation, I express herein my honest gratitude.

To Mr Cardoso (ADAI) and Mr Paulo (Volunteer Fire Brigade of Lousã), thank you for the help to create and obtain the experimental components required for this investigation.

My final appreciation goes to all the persons (in particular friends and high school teachers) who have contributed not only for the knowledge that I have nowadays but also for the motivational words and countless advice which I will always remember.

ABSTRACT

Been wildfires (WF) one of the most catastrophic mother nature events occurring around the world (regarding both human losses and destruction of forests), the relevance of the research on this phenomenon must not be disregarded.

Over the last decades, countless devices and solutions have been studied and developed with the aim to offer protection against wildfires, whether in the form of shielding of houses and other infrastructures, but also regarding personal protection to reduce the number of human fatalities. One of the solutions found was the creation of a fireproof barrier which could be placed in the boundary region between the forest and the urban areas (the so-called wildland-urban interface). This solution has the ability to sustain (definitely or, at least, for a certain period of time) the advance of the fire front, giving extra time which could mean the difference between the saving or the loss of human lives.

The present thesis was done within the project FireProtect. This project aims at developing, testing and demonstrating several protection systems for people and elements exposed to forest fires. One of such systems is a water-cooled fireproof barrier for the protection of infrastructures against forest fires. Taking into account the research work of Batista (2018), the present thesis further develops this topic and thus can be considered as an extension of this work.

The main objective of the present research study is the development of a prototype of an intelligent water-cooled fire-resistant barrier for fire front suppression with optimal water resource usage. Sustained by a theoretical model, this system was idealized to have the ability to vary the water mass flow rate required to ensure the full integrity of the surface of the barrier, according to the fire heat intensity at which the barrier is exposed. Laboratory experiments were also conducted to corroborate and adjust the theoretical calculations and validate the system.

Keywords wildfires, fire protection devices, fireproof barrier, wildland-urban interface, water cooling, water sprinklers.

RESUMO

Sendo os incêndios florestais um dos mais catastróficos eventos que acontecem na natureza (considerando a perda de vidas humanas e a destruição de florestas), a importância de cada estudo relacionado com este fenómeno deve ser tido em conta com o máximo de consideração.

Ao longo das últimas décadas, inúmeros equipamentos e soluções têm sido estudados e desenvolvidos não só com o objetivo de oferecer proteção a casas e infraestruturas, mas também considerando a proteção individual com o intuito de reduzir o número de vítimas mortais. Uma das soluções idealizadas é a criação de uma barreira antifogo que pode ser colocada na região entre a floresta e a área urbana (interface urbano-florestal). Esta solução tem a capacidade de impedir (definitivamente ou, no mínimo, for um determinado período de tempo) o avanço da frente de chama, dando deste modo, um tempo extra que pode ser a diferença entre a perda e o salvação de vidas humanas.

A presente tese é inserida no projeto FireProtect. Este projeto tem como objetivos o desenvolvimento, teste e demonstração de vários sistemas de proteção para pessoas e elementos expostos aos incêndios florestais. Um desses equipamentos consiste numa barreira antifogo refrigerada a água para a proteção de infraestruturas contra a destruição provocada pelos incêndios florestais. Considerando o trabalho desenvolvido por Batista (2018), a presente tese desenvolve mais este tópico e pode ser considerada como uma extensão do seu trabalho.

O principal objetivo desta investigação é o desenvolvimento de um protótipo de uma barreira antifogo refrigerada a água inteligente que tem a capacidade de se ajustar consoante a intensidade do fogo, com o intuito de otimizar o consumo de recursos.

Suportada por um modelo teórico, este sistema foi idealizado de forma a ter a capacidade de ajustar o caudal de água necessário para assegurar a integridade da superfície da barreira em função da intensidade de fogo que a barreira está exposta.

Ensaios laboratoriais foram igualmente realizados de forma a corroborar e ajustar o modelo teórico desenvolvido e analisar a viabilidade de todo o sistema.

Palavras-Chave Incêndios florestais, equipamentos de proteção a incêndios, barreira antifogo, interface urbana florestal, refrigeração a água, aspersores.

CONTENTS

LIST OF FIGURES

LIST OF TABLES

LIST OF SYMBOLS AND ACRONYMS

Symbols

$\dot{m}$ - film mass flow rate (kg/s.)

q'' - net radiative heat flux incident on the surface (W/m^2)

μ - dynamic viscosity of water (kg/m.s)

Bi -Biot number

C_p specific heat of the barrier (J/kg. K)

DT/dt- temperature differential per unit of time (ºC /s)

E radiative heat flux emitted by the surface (W/m^2)

G irradiation heat flux incident at the surface of the fabric (W/m^2)

Ha hectares

H_{comb} heat of combustion (J/kg)

H_{heat} height of the heater defined in Kabov investigation.

h_{mean} average convective heat transfer coefficient (W/m2. K)

$H_{vap.}$ enthalpy of vaporization (kJ/kg)

K_{water} water conductivity (W/m.K)

L_c characteristic length used in the *Lumped Capacitance Method*

$m_{col.}$ mass of water which falls down in the water basin(kg/min)

$m_{out.}$ mass of water lost (kg/min)

$m_{sp.}$ mass of water sprayed (kg/min)

$m_{vap.}$ mass of water vaporized(kg/min)

Nu – Nusselt number

Pr – Prandtl number

Q film volume flow rate (m^3/s)

q''_{conv} convective heat flux between the surface and the water film (W/m^2)

q''_{rad} net radiative heat flux at the surface of the fabric (W/m^2)

q_{conv} convective power between the surface and the water film (W)

q_{rad} net radiative power at the surface of the fabric (W)

Re – Reynolds number

$T_{(t)}$ safety temperature of the barrier (K)

T_∞ ambient temperature (K)

T_0 initial temperature of the barrier at which the cooling system is activated (ºC)

t_{exp} period of time at which the cooling system is in operation (s)

T_{fire} temperature of the fire plume (K)

T_{su} temperature of the surface (K)

WMC_{fuel} water moisture content of the fuel (%)

$\alpha_{barrier}$ absorptivity of the barrier

δ maximum height in a rivulet's cross-section defined in Al-Khalil investigation.

δ_{film} film thickness defined in Kabov investigation

ε emissivity of the surface

ν – kinematic viscosity of water (s/m^2)

ρ reflectivity of the barrier

$\rho_{barrier}$ density of the barrier (Kg/m^3)

τ_{rad} Stephan Boltzmann's constant (5.67×10^{-8} $W/m^2 . K^4$)

m mass of the barrier (Kg)

τ thermal time constant

Acronyms

ADAI – Associação para o Desenvolvimento da Aerodinâmica Industrial

IR- Infrared

LEIF – Laboratório Estudos de Incêndios Florestais

WF – Wildfires

WUI – Wildland Urban Interface

1. INTRODUCTION

Wildfires (WF) has one distinguishable characteristic when compared to all the others mother nature catastrophes (e.g earthquakes, hurricanes, tsunamis): when it begins, is the only natural phenomenon whose consequences can be minimized with the intervention of the human species.

A huge effort and countless studies have been made in order to analyse and understand such a complex phenomenon. Despite this effort, the number of wildfire victims all over the globe has been increasing. For this main reason, there is a need for a constant improvement of the scientific knowledge and safety systems which directly contribute to the protection of people and infrastructures against forest fires.

In Portugal, WF causes the destruction of thousands of hectares (Ha) every year. According to Pordata (2018), one can be concluded that since 2014 the total burnt area has been increasing in this country (Figure 1.1). However, considering Pordata (2018) it shows that the number of forest fires has been decreasing (Figure 1.2). These results mean that the destruction generated by WF is rising year after year.

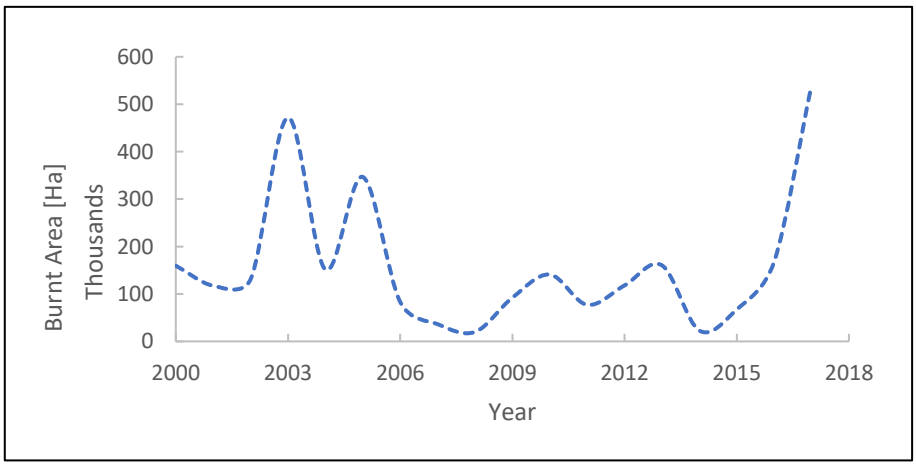

Figure 1.1 - Total Burnt area in Portugal from the years 2000 to 2017.

In Figure 1.1 shows that the most devastating WF season was in 2017 with a total burned area of 539 thousand Ha.

In that year, in the wildfire of Pedrógão Grande, a total of 64 persons lost their lives, being one of the most tragic events in the history of Portugal.

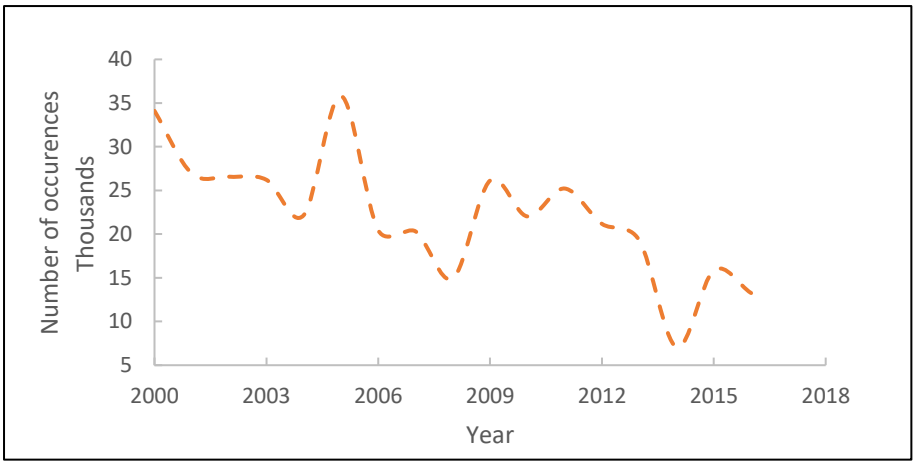

Figure 1.2 - Number of forest fires in Portugal between the years 2000and 2016.

According to Pordata (2018) and comparing the numbers between Portugal and the rest of the Europe, it can be seen that over the year of 2016 the highest total burned area (normalized by one hundred thousand square kilometres of land) was in Portugal with a value more than five times higher than the second-placed nation. In that year, the highest number of ignitions was also in Portugal with a value of 13 thousand occurrences.

1.1. State of the art

Over the years there have been countless inventions and mechanisms with the main purpose to protect firefighting vehicles, people and infrastructures against wildfires. In fact, there has been a great development in terms of firefighting safety, namely on high thermal resistance equipment for individual protection as well as systems for vehicles protection, such as water sprinklers. The critical area where most wildfire-related fatalities occur is in the wildland-urban interface (WUI), which can be defined as the region where forest and human infrastructures coexist. When a WF reaches such areas, people are directly exposed to its devastation, thus several protecting devices must be developed in order to defend people and their goods.

Typical protection systems usually consist of fireproof barriers made of high-temperature resisting materials. In some cases, water sprinkling is used to reduce the fabric temperature, thus ensuring a longer lifetime and effectiveness of these solutions. In this way, it is important to consider Smith & Smith (1988) which the main purpose is to keep safe a pre-established perimeter from high external temperatures (up to 980 ºC) using a vertical high resistant temperature fence (Figure 1.3).

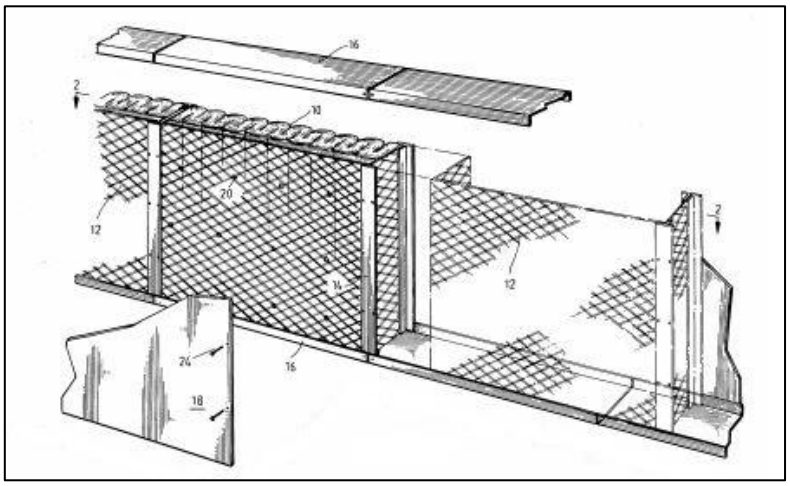

Figure 1.3- Smith's invention (adapted).

According to this publication, this invention was initially idealized to protect vaults having in their interior magnetic tapes and photographic films which could be damaged when exposed to a temperature more than 65.5 ºC.

The fact of this fence only depends on a single protective system without having any extra water sprinkler system, could mean that its efficiency is compromised when exposed to high radiant heat for a prolonged time.

For infrastructure protection (namely residential and industrial buildings), many patents were created to safeguard critical areas (such as windows, doors and roofs) using for that purpose water sprinklers-based systems. These devices allow not only direct protection when a WF is nearby, but also when incandescent flying particles from long-distance fires reach the protected area. In this way, it could be interesting to consider the creation of Gelaude (1984). In this patent, it is described an automatic sprinkler-based system which is activated to protect a pre-established perimeter when it detects a sudden rise in the ambient temperature. In Figure 1.4 it is shown a schematic representation of this system.

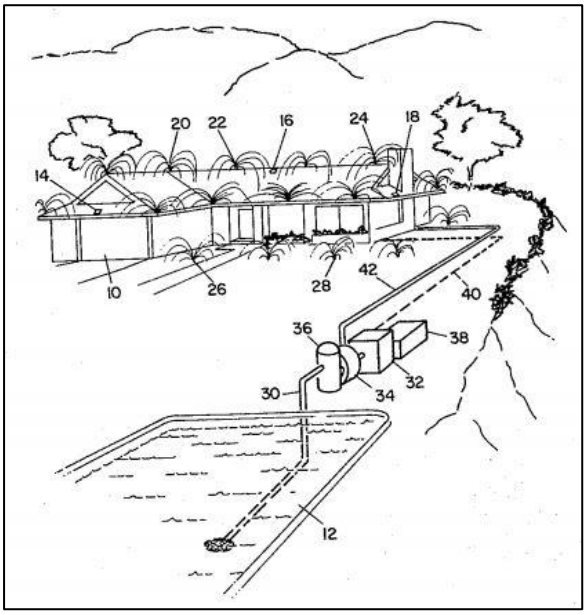

Figure 1.4 - Scheme of Gelaude invention (adapted).

Connected to a nearby water source (swimming pool or local water supply), it also allows to adjust the water flow rate in order to shield the perimeter and, at the same time, optimize the consumption of water.

The use of water sprinklers systems to protect structures against WF was considered in the creation of Orrange & Sweeton (2002). This device is based on rotating water sprinklers mounted on the roof of the protected building (Figure 1.5). Comparing this

system with the invention of Gelaude (1984) it can be deduced that, having spinning sprinklers allows a higher perimeter projection and, consequently, the possibility of increasing the moist of surrounding combustible material (trees and shrubs).

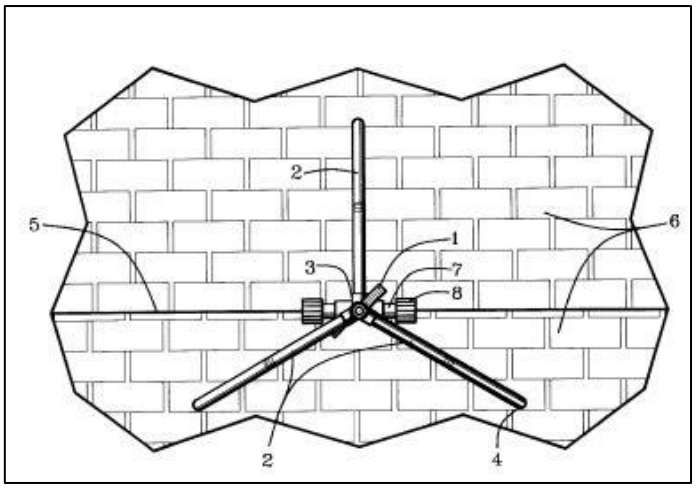

Figure 1.5- Orrange & Sweeton rotating sprinklers invention.

In terms of water-cooled based systems, several studies were conducted in order to analyse the behaviour of water and spray films exposed to fires. Due to its thermal properties and availability, water (in form of mist or spray) has always been preferentially used to suppress fire. Having a relatively high enthalpy of vaporization ($H_{vap.}$) and high specific heat (C_p) it allows the absorption of a great amount of heat before its vaporization. In this way, it is convenient to take into consideration the work of Buchlin (2005). In this investigation it was analysed the performance of an active water spray curtain for petrochemical industry application. In Figure 1.6 is represented the field tests that were conducted.

In the laboratory experiments, it was also tested industrial nozzles with water mass flow rates up to 1 kg/s (corresponding to a water pressure of 8 bar). To simulate a heat source, propane burners were employed.

The fact of only having one suppression system against fire (without any physical barrier) could lead to a minor effectiveness when compared to a system that has combined the two mechanisms.

According to Buchlin (2005) field tests, in order to reach attenuation values up 75%, the water mass flow rate per meter of water curtain shielding was 2 kg/s, which requires an enormous water storage tank in order to operate for a prolonged time.

Figure 1.6- Buchlin field experiments.

In the investigation of Meredith, De Vries, Wang, & Xin (2012), it was studied the efficiency of cooling a vertical stainless steel plate, which is exposed to external radiation from a heated plate, using a water-film system. The main goal of this work was to analyze the influence of the water-film mass flow rate on the radiative heat flux measured on the surface of the plate as well as the temperature distribution. As can be seen in Figure 1.7, at the bottom of the target plate, it was placed a stainless-steel basin which could collect the excess of water.

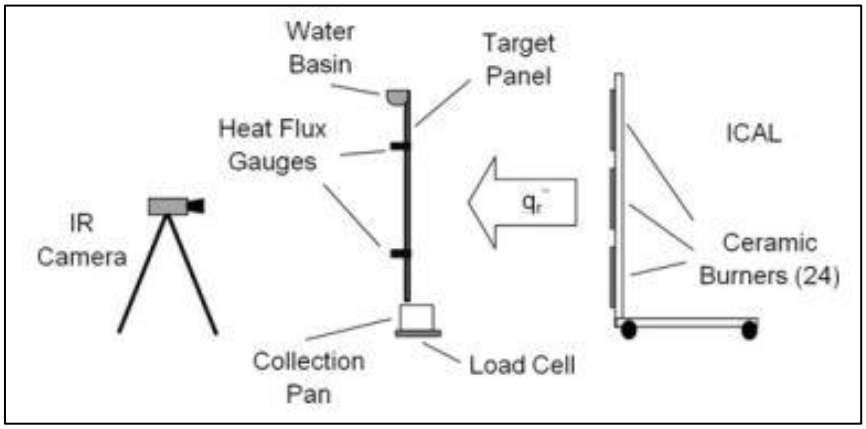

Figure 1.7 - Experimental setup used on Meredith tests.

In order to simulate a fire radiation environment, the range of radiation used in this investigation was between 5 to 33 kW/m^2.

In all the experimental tests it was verified that despite having a water-film flowing down the stainless steel surface, it always occurred a formation of dry zones and rivulets paths along its surface. This fact means that having a relatively high water film mass flow rate could be insufficient to maintain the surface temperature below a critical value.

Using a fire growth model with fundamental film transport equations for mass continuity, momentum and energy, theoretical calculations were also made to corroborate the experimental results. This comparison can be seen in Figure 1.8.

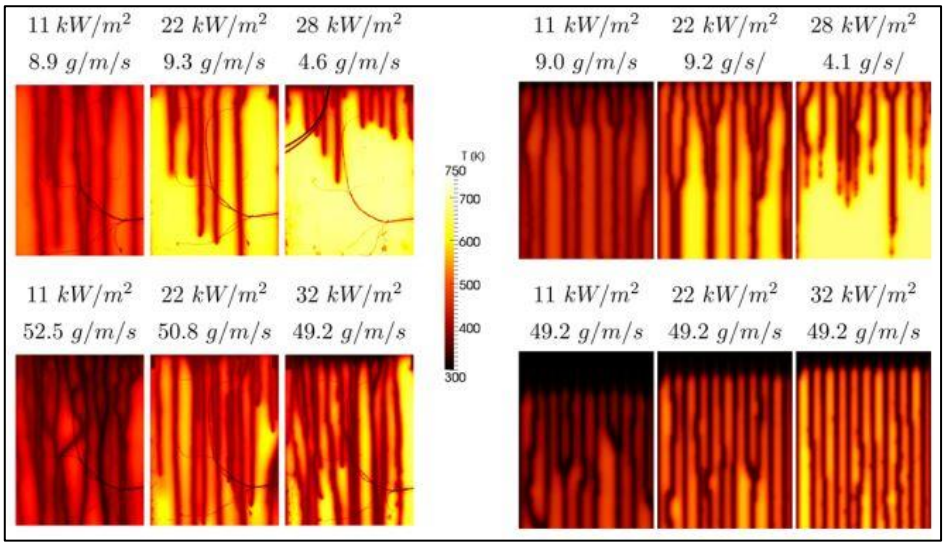

Figure 1.8 – Experimental values (on the left) and theoretical predictions (on the right) in Meredith tests.

By analysing Figure 1.8 one can be concluded that for the same conditions (water mass flow rate of 49.2 g/m.s and radiation heat flux of 32 kW/m^2) the heat transfer model can simulate with precision the experimental results.

Having some similarities with the investigation of Meredith et al. (2012), the main difference between this study and the investigation of Lev & Strachan (1989) relies on the theoretical modelling used and the study of different types of nozzles (mist and spray).

In this study, a two-meter square radiation furnace was used to simulate a fire front. This equipment could reach a maximum radiant heat flux up to 90 kW/m^2 and water mass flow rates used were between 1.6 and 21.2 L/min.

In Figure 1.9 is shown the experimental apparatus.

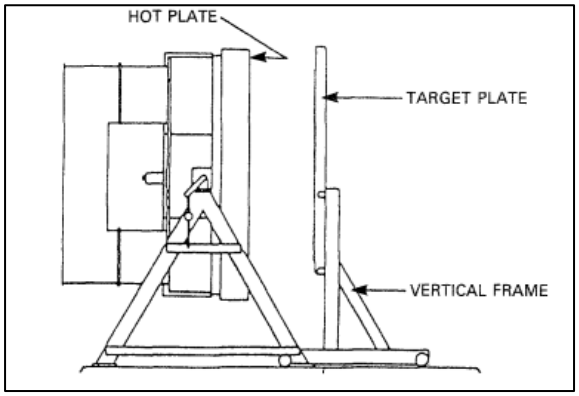

Figure 1.9 – Experimental setup used in Lev and Strachan experiments.

Additionally, theoretical calculations were also considered with the aim to confirm practical results. Considering that heat loss (to the surroundings) represented 5% of the total energy generated in the hot plate and the radiating panel acts like a black body, the calculated values had an insignificant difference when compared to the practical results (cf Figure 1.10 and Figure 1.11).

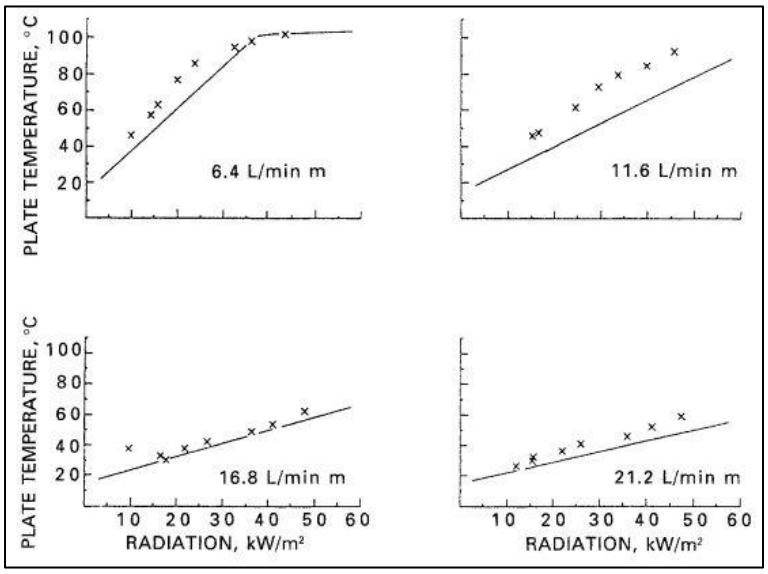

Figure 1.10 - - Evolution of target-plate temperatures as a function of radiant heat flux and water-spray flow rate. Crosses represents experimental results and solid line represents model projected values.

Regarding film-cooling conditions, measured results were often higher than the theoretical predictions which could be related to an uneven wetting of the target plate.

Considering Figure 1.10 and Figure 1.11, it can be concluded that by using any type of water-cooling system (spray or mist) and using the lowest flow rate tested for each system, it can lead to a maximum temperature of the target-plate of 100ºC.

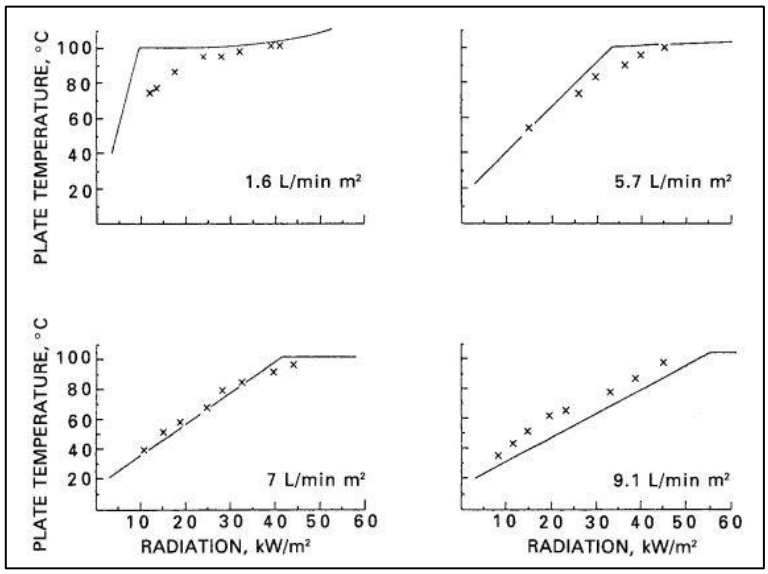

Figure 1.11 - Evolution of target-plate temperatures as a function of radiant heat flux and water-mist flow rate. Crosses represents experimental results and solid line represents model projected values.

However, maximum temperatures well above 100ºC were also achieved in special conditions (minimal flow water rate combined with winds). For the tests which were used the maximum water mass flow rate (21.2 and 9.1 L/min.m^2 for film and mist, respectively) one can conclude that mist type nozzle is less effective when compared to the spray type. Although the values of water mass flow rate for the two cooling systems considered was not the same, it can be verified that the temperature growth rate is more accentuated for spray type when compared to mist type conditions.

1.2. Motivation

In Portugal, particularly in the beginning of every summer season, the government and the media usually releases several recommendations for the population to

have extreme cautions and adopt responsible behaviours to prevent the ignition of a WF. Despite all warnings, every year the numbers of wildfires and area burned are keep rising. Being prevention, the principal strategy adopted, it can be easily seen that it is not enough. There is a need to conceive devices and systems, based on acquired scientific knowledge regarding fire behaviour, which could offer more protection for people and infrastructures in the WUI.

By looking at the most relevant systems based on water-cooled fire-resistant fabrics, one can conclude that there is an opportunity for improvement and for the development of a complete fire protection solution, having both a fireproof fabric and a water sprinkler system to protect and cool a fire-resistant barrier, which could ensure not only an extra lifetime of the fabric but also been able to shield against higher radiation values when compared to a system with only one of the two systems considered.

Finally, such research work for the efficiency of a water-cooled fireproof barrier for wildfires has never been done before in the scientific community, thus it presents many challenges which are worthy of addressing and pursuing the sake of knowledge.

1.3. Objectives

This research work aims at the development and implementation of an intelligent fire-resistant water-cooled barrier, which scheme is represented in Figure 1.12.

The main objective of this research work was to understand the complex mechanisms behind water cooling phenomena of surfaces exposed to very high-intensity heat sources, more specifically fireproof fabrics which are exposed to a fire front. To accomplish this research work, several key actions were performed:

1. Thorough research and analysis of the state-of-the-art regarding water-cooled fire barrier systems. Patents and inventions of fireproof devices and respective operational characteristics were also taken into consideration;

2. Thermal modelling of the most important physical phenomenon which occurs in the barrier when a radiation heat source is placed next to it. Convection heat coefficients and the water mass flow rate required to counterbalance the heat flux incident on the barrier were calculated and estimated;
3. Laboratory experiments to validate the theoretical model were also performed.

The knowledge obtained can then be used and implemented in an intelligent fire-resistant water-cooled barrier, for the protection of people and infrastructures, with optimal usage of resources.

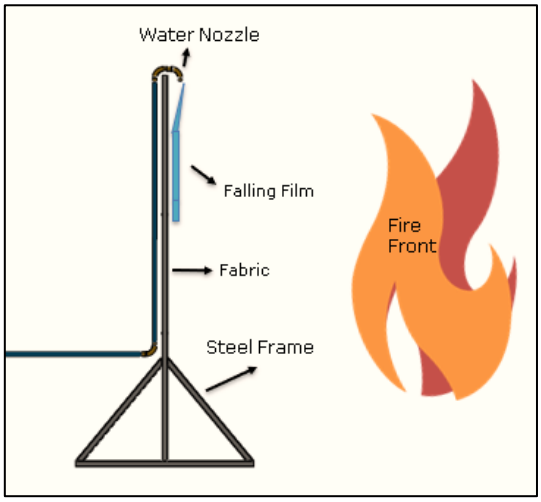

Figure 1.12 - Illustration of the proposed solution.

1.4. Outline

This dissertation document is organized in five main chapters.

In the first chapter, it is described the state of the art as well as the motivation and the objectives which the present investigation pretends to accomplish.

In the second chapter, it is presented the modelling of the phenomena occurring in the surface of the fireproof barrier. This theoretical approach is then validated by the experimental work which is detailed in the third chapter.

The realization of laboratory tests was vital to confirm and adjust the assumptions initially made in theoretical modelling. Comparisons between the predicted values and the experimental results are described in the fourth chapter.

The fifth chapter is devoted to the main achievements obtained in this dissertation as well as some suggestions regarding further research on this topic.

2. HEAT TRANSFER MECHANISM MODELLING

2.1. Description

A fireproof barrier can be described as a flexible textile material whose main purpose is to protect against the extreme values of radiation and temperature from an adjacent fire. Currently, there are several worldwide manufactures with numerous kinds of fireproof barriers available on the market, each one made of different fire-resistant materials which lead to different performances when exposed to an extreme heat source.

The main component which the fireproof barriers tested in this investigation are made is fibreglass type E filaments with an aluminium layer covering its surface. This type of fibreglass in particular can be highly effective when exposed to extreme radiation and temperature due to its high reflective and temperature resistant properties.

As described previously, one of the main objectives of this investigation is to conceive a theoretical model which estimate the necessary water mass flow rate in order to ensure the maximum possible protection of the fabric. The value of the water mass flow rate required will be dependent of several parameters, such as the instant temperature of the barrier and its pre-established critical temperature, the total incident heat flux on the surface and, most importantly, time of exposure. In fact, considering that fire is an extreme transient phenomenon (with instant changes of temperature and radiation heat flux generated), the conception of a theoretical model will be sharply difficult.

Even though this strongly time-dependent behaviour of the fire, a heat balance to the barrier has to be estimated and therefore, the complexity inherent to a fire event can be decomposed into much simpler equations which can be easily interpreted.

Regarding also the study of several types of water spray nozzles and the respective practical (and theoretical) influence in the fabric resistance to radiation, the present investigation will be an enormous progression in this topic.

2.2. Heat Fluxes

It is known that there are three main ways to transfer heat from a system to another: conduction, convection and radiation. For this particular study, since the main area of analysis is the interface region between the surface of the barrier and the water film falling down through its surface, only the heat flux in the form of conduction will not be taken into consideration for the final results. In fact, since the maximum temperature reached at the barrier will always occur in the side with the exposure to the flames, the temperature profile thought the barrier thickness and the temperature measured in the backside will be dependent of the heat flux interactions between the water film, the fire and the front side surface. A schematic representation of the heat fluxes that were considered in this investigation is shown in Figure 2.1.

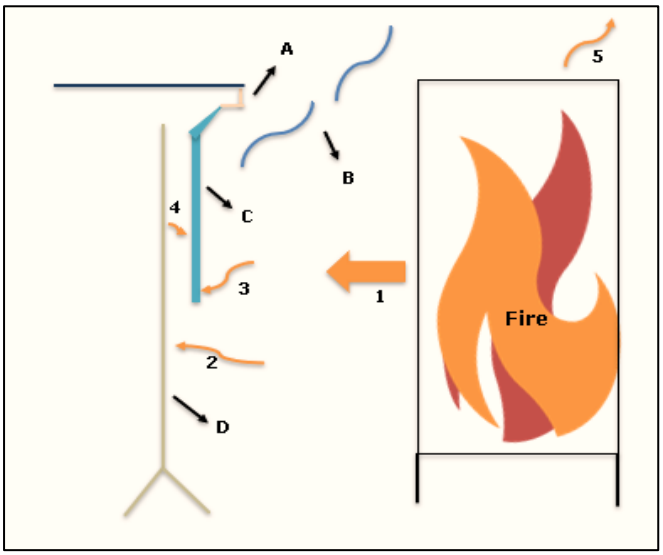

Figure 2.1 - Scheme of the heat fluxes considered.

The legend used in Figure 2.1 can be consulted in Table 2.1and Table 2.2.

Reference	Description
A	Water nozzle
B	Water vaporized
C	Water film
D	Fabric

Table 2.1 - Legend the main elements used in the experiments.

Reference	Description
1	Total heat flux generated in the fire
2	Total heat flux incident in the fabric
3	Radiative heat flux generated by the fire and absorbed by the water film
4	Convective heat flux between the fabric and the water film
5	Total heat flux generated by the fire to the surroundings

Table 2.2 - Legend of the heat fluxes considered.

2.3. Lumped Capacitance Method

Regardless of the size of the fire plume, it is well known that fire is a transient chemical reaction with instant variations in the value of temperature reached and heat flux generated. In fact, besides the natural behaviour of fire itself, there are several variables which have an important role in fire growth. Parameters such as wind velocity and direction, relative humidity and temperature of the air, type of fuel and respective characteristics (mass load and moisture content), and topography can be considered the main variables which could affect fire development.

Since this natural event is a complex phenomenon, all over the years there has been made countless investigations regarding fire suppression environments using water. For most of these investigations, the main purpose was to examine the effect of a water-spray film falling down a vertical hot surface simulating a fire suppression situation. In fact, one particular investigation has been able to reach some interesting correlations and final conclusions regarding the value of water mass flow rate required as a function of the incident heat flux (Meredith et al. (2012) for both experimental and theoretical approaches. Although the maximum incident heat flux on the target plate reached values up to 33 kW/m^2, this investigation does not consider the transient phenomena associated in fire situations.

The fabric overall temperature can be expressed by the general heat flux balance represented in Equation 2.1:

$$m * Cp * \frac{dT}{dt} = q_{rad.} - q_{conv.}$$

Equation 2.1

In order to estimate the value of the heat flux incident on the surface of the barrier, it was used the definition of *net radiative flux* (Incropera, Bergman, Lavine, & Dewitt (2011) defined in Equation 2.2:

$$q_{rad.} = G - \rho * G - E = \alpha * G - E$$

Equation 2.2

It the present research study it is defined that ρ is the fraction of the irradiation that is reflected and α is the fraction of the irradiation that is absorbed. Considering that both the heat fluxes released from the barrier and from the fire plume can be obtained using the *Stephan Boltzmann law for radiation* and considering that the fire plume acts like a blackbody (according to Buchlin (2005) and Lev & Strachan (1989)), Equation 2.2 results in Equation 2.3.

$$q''_{rad.} = \alpha * \left(\tau_{rad.} * {T_{fire}}^4\right) - \left(\varepsilon * \tau_{rad.} * {T_{su.}}^4\right)$$

Equation 2.3

Although the exact values of α and ε are still unknown, for the theoretical simulation it was supposed that they assume the values of 0.8 and 1, respectively. For the convective heat flux term, it was used *Newton's law* for cooling (cf. Equation 2.4):

$$q''_{conv.} = h_{mean} * \left(T_{su.} - T_{fire}\right)$$

Equation 2.4

One can conclude that the value of h_{mean} is one of the coefficients which require more effort to obtain. In fact, there is a countless list of both empirical and theoretical correlations with the aim to obtain the value of the average heat transfer coefficient for practically all kind of situations. For thin-film conditions and according to Al-Khalil, Keith, & De Witt (1991) the value of the average heat transfer coefficient for a water film falling down a vertical surface can be given by:

$$Nu = \frac{h_{mean} * \delta}{k_{water}} = 3.2 + 2.37 * 10^{-4} * Re$$

Equation 2.5

In Equation 2.5, Re can be calculated by $Re = \dot{m}/\mu$. By analysing the correlation of Al-Khalil et al. (1991), it can be seen that, for relatively low values of water mass flow rates, the value of Nu has an insignificant dependence on Re. In fact, for the experimental setup idealized, it is expected that the maximum water mass flow rate available for the water spray nozzles is about 3.2 L/min and, consequently the value of Re is 59.8 (considering an average temperature of water of 25ºC). This value of water temperature was the value obtained through the IR measurements. Inserting this value of Re in the Equation 2.5 it results for the value for Nu of 3.21. Once this calculation was made considering the maximum water mass flow rate available, it can be concluded that the correlation of Al-Khalil et al. (1991) is not appropriate for this research study.

One approach which could lead to satisfactory results is the *Lumped Capacitance Method* for transient conduction situations. Using *Bi* to test its validity, this method could give the value of h_{mean} as a function of well-known parameters. However, in order to use this method and according to Incropera et al. (2011), it must be assumed that the temperature of the fabric is spatially uniform. As we can see from Batista (2018), when the barrier is exposed to radiant heat flux from a fire, it can be observed that the fabric has temperature gradients along its entire surface and this fact cannot be ignored.

Although the existence of temperature gradients in the surface of the barrier, in order to use the *Lumped Capacitance Method*, it was assumed the worst-case scenario. This situation can be defined as all the surface of the barrier exposed to the fire is at the maximum temperature recorded by the thermocouples. By simulating the performance of the entire

system using this assumption, the final results could be an overestimation calculation when compared to the experimental results. In Incropera et al. (2011) it can be seen that the *Lumped Capacitance Method* can be expressed as:

$$\frac{T(t) - T_{\infty}}{T(0) - T_{\infty}} = \exp(-\frac{t_{exp.} * h_{mean}}{\rho_{bar.} * C_p * L_c})$$

Equation 2.6

The value of τ can be defined by the quantity:

$$\tau = \frac{\rho * C_p * L_c}{h_{mean}}$$

Equation 2.7

Take into consideration that the value of T(∞) is irrelevant when compared to the value of T(0), the quotient of the left side of Equation 2.6 can be expressed as a function of $T(t)$ and $T(0)$. By reorganising Equation 2.6, h_{mean} can be expressed as:

$$h_{mean} = -\frac{\rho * C_p * L_c}{t_{exp.}} * \ln\left(\frac{T(t)}{T(0)}\right)$$

Equation 2.8

Using Equation 2.8 it is possible to obtain the value of h_{mean} as a function of well-known physical properties of the fabric and some measured values. For a wide range of t_{exp} it could be interesting to analyse the dependence of this variable in the value of h_{mean} (Figure 2.2). For the value of C_p it was assumed value of 844 J/kg. K (according to Batista (2018) tests). It was considered a value for m of 520 gr/m^2. By analysing Figure 2.2, it can be concluded that as the value of $t_{exp.}$ increases, the required value for h_{mean} decreases for each temperature considered. This behaviour is coherent with the expectations.

In fact, predicting the values of h_{mean} for a certain value of $t_{exp.}$ and 2 $t_{exp.}$ it is understandable that the value corresponding to 2 $t_{exp.}$ is lower. Once the barrier is affected by the cooled water during a much longer of time the value of h_{mean} required for the same temperature difference is lower. Having obtained the value of h_{mean}, the determination of DT/dt is now possible.

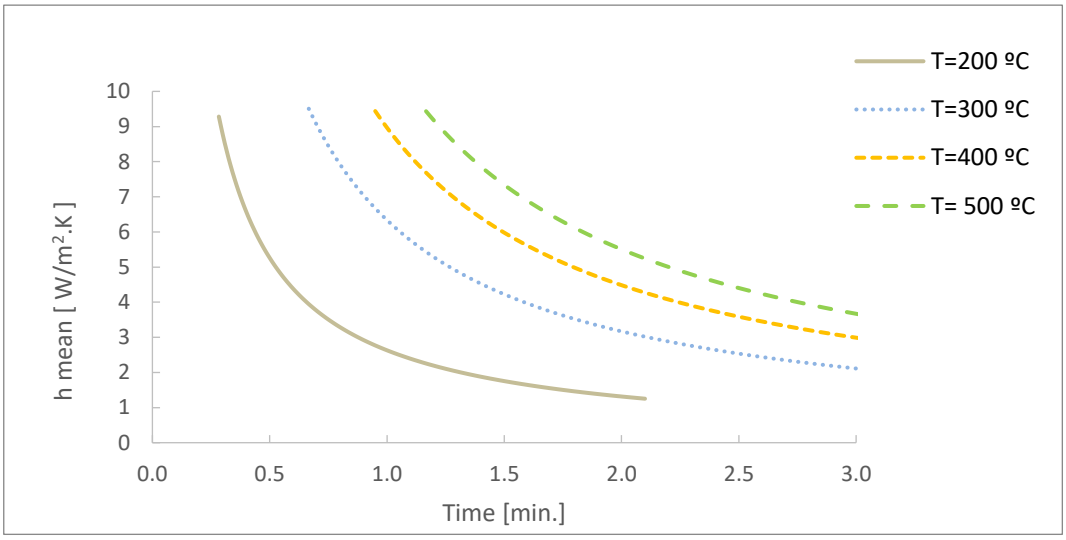

Figure 2.2 – Convective heat transfer coefficient as a function of time at several initial temperatures of the fabric.

The dependence of DT/dt as a function of. t_{exp} can be analysed in Figure 2.3.

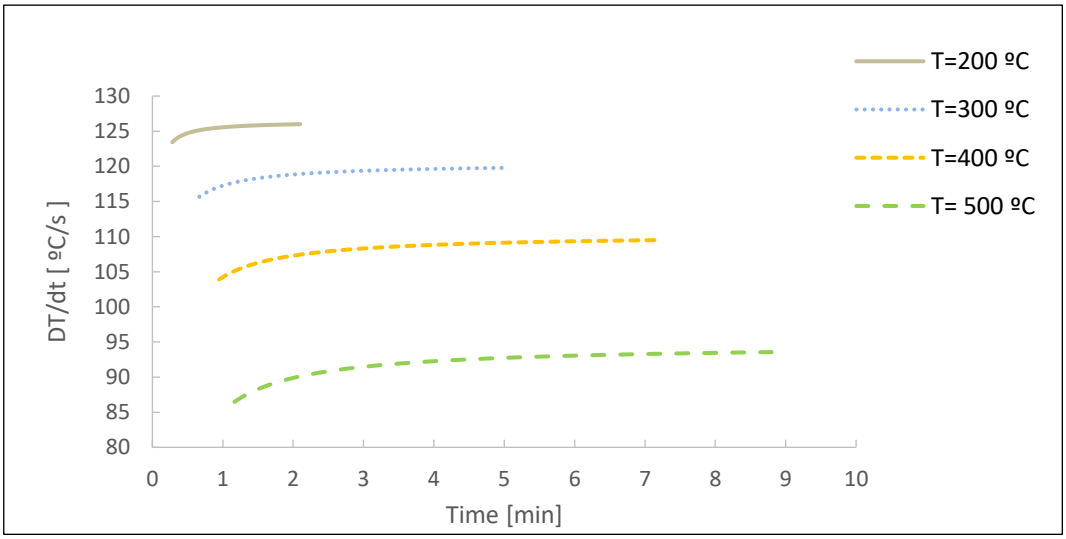

Figure 2.3 – DT/dt as a function of time at several initial temperatures of the fabric.

It was considered that the temperature of the fire was constant and equal to 850ºC. Comparing the behaviour of DT/dt in terms of $t_{exp.}$, one can concluded that for the situation at which the temperature of the barrier is higher (with all the remaining variables being constant) the stabilized value of DT/dt is lower when compared to the situation regarding a lower value for the temperature of the barrier (Figure 2.3). This fact can be justified by the heat balance between the fabric and the fire. For the situation at which the temperature of the fabric is higher, the temperature growth until the thermal equilibrium is lower when compared to the situation at which the temperature of the fabric is considerably lower than the temperature of the fire.

Although the achievement of both empirical and theoretical correlations which can give the value of h_{mean} as a function of known parameters, the dependence of the value of the water mass flow as a function of h_{mean} is still undetermined. Even though there are a great amount of correlations involving several adimensional parameters, including *Nu*, *Re* and *Pr*, there are a small number of correlations which could be applied to this research study. Besides, the value of the water mass flow rate used in the present investigation is relatively low with a corresponding low value of Re. Consequently, some of the thin film correlations found are not suitable for simulating these phenomena. Nevertheless, according to Kabov, Diatlov, & Marchuk (1995), Equation 2.9 could be applied for a laminar thin film falling down a vertical surface with the condition of the incident heat flux being constant.

$$\left(\frac{(\frac{Nu}{2.06})^4 - 1}{0.0443 * (2 * Pr * \frac{\delta_{film}}{H_{heat.}})^{\frac{4}{3}}.} \right)^{\frac{3}{4}} = \frac{Q}{\nu}$$

Equation 2.9

To use Equation 2.9 in the theoretical modelling, it was made some adjustments to the original equation. Once the values obtained for the δ_{film} were almost insignificant, this value was replaced for the L_c.

In the present research study, the value of L_c and H_{heat} were considered equal to the height of the fabric (i.e. 1 meter). In this way, the real equation used in the theoretical modelling was:

$$\left(\frac{(\frac{Nu}{2.06})^4 - 1}{0.0443 * (2 * Pr * \frac{L_c}{H_{heat.}})^{\frac{4}{3}}.} \right)^{\frac{3}{4}} = \frac{Q}{\nu}$$

Equation 2.10

In Equation 2.10, *Nu* can be defined as:

$$Nu = \frac{h_{mean} * L_c}{k_{water}}$$

Equation 2.11

Combining Equation 2.8, Equation 2.10 and Equation 2.11, a single correlation between the value of Q as a function of $t_{exp.}$ can be obtained (Figure 2.4).

In Figure 2.4, it can be confirmed the predictions: in a worst-case scenario (i.e. when the temperature of the barrier is higher) it would be necessary a higher value of h_{mean} (and, consequently, a higher value of Q) when compared to a condition when the temperature of the fabric is lower.

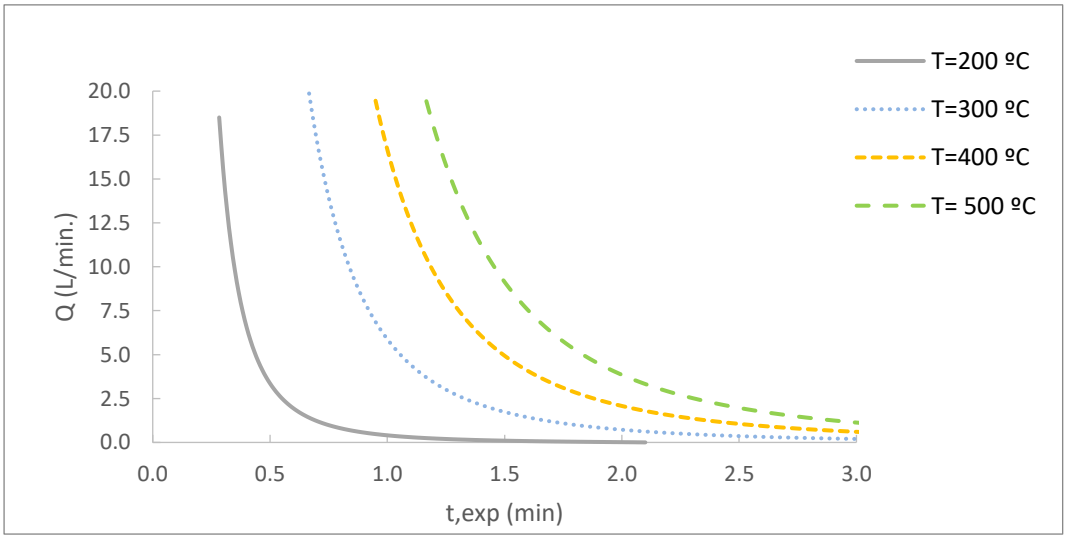

Figure 2.4 – Water mass flow rate values as a function of time, at various initial temperatures of the fabric.

Despite the achievement of Equation 2.10 it is imperative not to disregard the validity of the *Lumped Capacitance Method*. According to Incropera et al. (2011), this method is only suitable for cases when Bi is less than 0.1. In fact, for values of $t_{exp.}$ less than 30 seconds, *Bi* is higher than the critical value and the Equation 2.10 cannot be applied. However, since the value of Q at which corresponds to the critical value of *Bi* is extremely high (in order of 40 L/s), Equation 2.10 is acceptable for the range of mass flow rate use in this research study. Moreover, for the maximum available value of Q, the magnitude order of *Bi* is 10^{-2} which is quite below the critical value.

Considering, for one particular situation, that the water spray nozzle is running at its maximum capacity of water mass flow rate, the temperature of the fire reaches the highest predicted values (850ºC), and assuming the initial temperature of the surface of the fabric of 200 ºC, it could be interesting to analyse the behaviour of the cooling system in such extreme circumstances. The maximum water mass flow rate available for the experimental tests was 1.71 L/min (considering ρ_{bar} equal to 1000 kg/m^3) and the corresponding maximum value for h_{mean} is 4.20 W/m^2. K. In these conditions, the value simulated for $q''_{conv.}$ is 1.62 kW/m^2. Comparing this result with the value simulated for the total radiative heat flux incident at the surface of the barrier (around 69.3 kW/m^2) it can be seen that despite using a relatively high-water mass flow rate value it is not sufficient to provide the necessary cooling effect to the fabric in order to ensure its full integrity during a reasonable period of time.

In addition, the difference between the values for DT/dt with the water system activated and the water system deactivated is 1.3ºC/s. This fact leads to the conclusion that, according to the model, the effect of using a water spray cooling system running at its full capacity to ensure the protection of the fabric is minimal.

3. EXPERIMENTAL APPROACH

3.1. Description

In order to evaluate the performance of the fabric with a water-cooling system when it is exposed to a high-intensity fire front, it was idealized an experimental setup which could simulate this scenario (Figure 3.1).

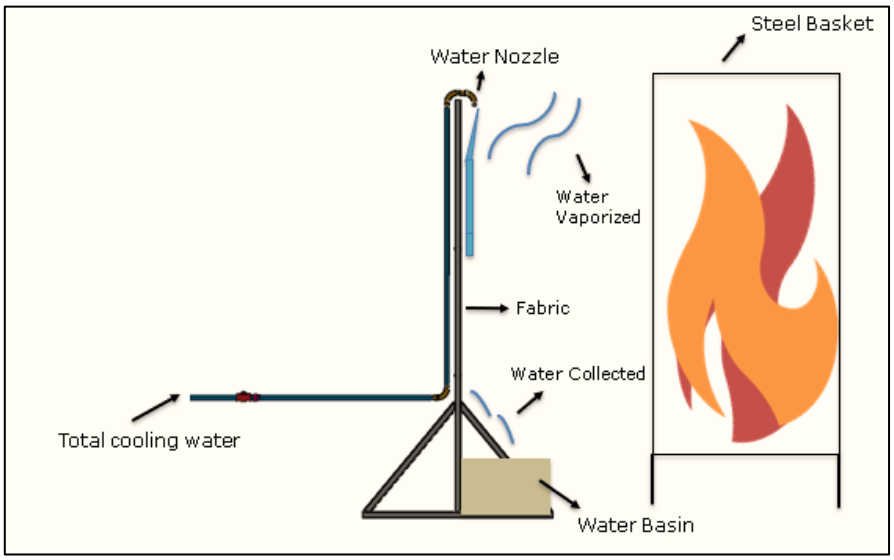

Figure 3.1 - Experimental apparatus idealized for the experimental tests (lateral view).

In the present investigation, it will be implemented an approach to simulate a fire front using a 3D fuel configuration (similar to the laboratory tests described in Soares (2018)). The fuel will be restricted in a steel made basket whose total volume is 0.5 m^3. In this way, it can be possible to simulate a real fire circumstance as well as reducing the fire intensity (compared to the values measured in Batista (2018)) due to the minor dimensions of the fabric. For all the experimental tests (1st and 2nd phase), the dimensions of the fabric were 1 meter heigh for 1.3 meter length. The ability to vary the distance between the fuel basket and the fabric allows to modify the total heat flux incident on the surface of the barrier and consequently analyse the performance of the system in various exposure conditions.

The fireproof fabric is fixed to a steel frame using several bolts, which help maintain it perfectly stretched. For safety and technical reasons, the water-cooling circuit was located behind the fabric to ensure that only the water nozzle and the falling water film are exposed to the fire. In the present research study, it was considered that the front side of the barrier is the side exposed to the flames.

In order to simulate a high-intensity fire front, it was used the combustion of forest fuel (shrubs and eucalyptus leaves) inside a steel basket. This experimental assembly was placed in front of a combustion tunnel with two large ventilators, capable of generating airflow speeds of up to 5 $m.s^{-1}$. This airflow is also used to increase the heat flux incident on the surface.

Depending on the type of nozzle, spray or atomizer, the fabric cooling mechanism works by spraying a water spray to the top part of the fabric or the space between the fabric and the fire front, respectively. The water that is sprayed to the top part of the fabric then falls, by gravity, covering and cooling the entire area of the fabric. A certain amount of the water is evaporated during the process and the rest reaches the floor, where it is collected in a water basin, placed below the steel frame structure. Part of the water falls outside the basin and is quantified in experiments without fire. The mass of the water collected in the basin at the end of each experiment is measured. In this way, it is possible to estimate the amount of water that is vaporized during the experiment, by knowing the total amount of water that was sprayed, the mass of water collected in the basin and the mass of water that fell outside the basin.

3.2. Standards

Once the fundamental purpose of the present thesis is the study of the behaviour of a fireproof fabric when it is exposed to a fire front, it was necessary to seek for the European standards which could be applied in this research study. In this way, not only the experimental methodology is well described and recognized by the scientific community but also, the final results could be compared to other investigations which followed the same procedures.

With the aim to certificate the protection of construction elements against indoor fire, it could be interesting to consider:

- EN 1363-1 (RISE Research Institutes of Sweden (2017)) describes a method to estimate the performance of any kind of construction element (walls or ceilings) when it is exposed to a pre-defined value for heat load and pressure

This standard provides the methodology to quantify the capacity of an element, or construction, to withstand high temperatures using a 3 x3 m^2 or a 5 x3 m^2 (depending on the size of the element tested) opening furnace. The standard also describes the measuring equipment which is used as well as the accuracy requirements for the measurements.

- ASTM E814 - 13a (ASTM (2017)b) delineates a procedure in order to test the behaviour of firestop systems installed in walls or ceilings.

The standard ASTM E814 - 13a(2017) can be used to determine the behaviour of a firestop system (mounted in fire-resistant walls or floors) when it is exposed to a pre-defined time-temperature fire test. At the end of each experiment it is evaluated the number, type and size of breaches which resulted from the test.

Regarding the protection in exterior fire situations it is crucial to take into consideration:

- ASTM E2707 – 15 (ASTM (2015)) defines a method to measure the performance of a system (exterior walls or similar) to avoid fire incursion when it is exposed to a direct flame.

This test method describes a procedure to evaluate the ability of the exterior wall covering element to sustain the progression of a specific fire exposure conditions. It is also mentioned the possibility of using an (IR) camera positioned at the protected side to measure the temperature profile of the surface and localize the existence of hot spots.

- ASTM E2307 – 19 (ASTM (2019)) describes the methodology for determinate the fire resistance of perimeter fire barrier regarding the ability to avoid fire progression.

This procedure consists of measuring the performance of a fire-resistant fabric, located at the protected side of an exterior wall or floor assembly, to resist at the passage of flames and hot gases. Transmission of the total heat through the fire barrier is also determined.

- ASTM E2748 - 12a(2017) (ASTM (2017)a) establish guidelines for the measurement of the behaviour of materials when exposed to fire under controlled conditions.

This guide defines a procedure to evaluate the behaviour of materials, products, or assemblies to heat and flame under pre-defined conditions. The final results obtained are suitable for general fire research as well as potential information to use on fire modelling software.

Once it was not possible to obtain the complete description for each standard, all the descriptions mentioned consists of a summary of the abstract of each norm. In spite of the existence of a numerous list of standards regarding fire protection systems, by comparing the objectives of the standards with the present investigation, it can be concluded that only the standard ASTM E2748 - 12a(2017) could be interesting to consider.

3.3. 1st Phase: Tests without fire

This first experimental phase was used to obtain results to serve as a reference for 2nd phase tests. In this phase, neither fire or forced airflow was used. The parameters which will be monitored in this phase can be compared with the results for the tests with fire (2nd phase tests) and allow to compare and analyse the performance of the system on different fire scenarios.

In this phase, two main types of water spray sprinklers were used: water spray curtain and atomizer. Each category was represented by two water nozzles which main difference relies on the water mass flow rate available for the same working pressure. In Figure 3.3 to Figure 3.4 are shown all the water nozzles tested.

Figure 3.2 - Nozzle CW_01 (spray type).

Figure 3.3 - Nozzle CW_02 (spray type).

Figure 3.4 - Nozzle AT_01 (atomizer type).

Figure 3.5 - Nozzle AT_02 (atomizer type).

In order to ensure that all the water nozzles are tested in the same conditions, it was kept constant both the values of the water pressure and the duration of each trial (Table 3.1). Moreover, it was made two series of tests: one series at the outside of the laboratory, and the second series at the inside.

Parameter	Value	Units
Water Pressure	3	bar
Time	1	min

Table 3.1 - Pressure and time duration of 1st phase tests.

The parameters which were measured in this phase were:

- Water mass sprayed for each nozzle ($m_{sp.}$)

With the aim to calculate the total water mass flow rate, it was used a 5-litter bottle to collect all the water which were debited from each nozzle, a weighing machine and a stopwatch. In order to ensure that the water pressure was kept constant since the beginning until the end of each nozzle test, it was followed the subsequent stages:

1. With the circuit valve closed, it was gradually established the velocity of 1800 RPM at the water pump (corresponding to a pressure of 3 bar).
2. When the water pump reached the desired pressure, it was placed the nozzle inside of the bottle, opened the circuit valve and initiated the stopwatch.
3. When the stopwatch reached 1 minute, the circuit valve was closed and immediately the water pump was turned off.
4. In the end, it was measured the total mass of water inside the bottle.

- Water mass collected ($m_{col.}$) and lost ($m_{out.}$)

Despite the presence of a water basin, there is always a certain amount of water that falls outside the basin reaching the ground. This amount of water that is not collected in the basin must be quantified in order to accurately estimate the mass of water vaporized during the fire experiments.

In order to measure the value of the mass of water that falls outside the water basin (considered as lost), it was adopted the following procedure:

I. For each type of spray nozzle analysed in this investigation, it was measured the total mass of water which was released from the sprinkler during a certain pre-established period of time ($m_{sp.}$);

II. Using a load cell, it was measured the final water mass inside the water basin ($m_{col.}$);

III. The difference between the values of $m_{sp.}$ and $m_{col.}$, gives an estimation for the mass of water which fell outside the water basin ($m_{out.}$).

- Water area coverage.

Using an IR camera, it was possible to evaluate the real area of the barrier covered by water and consequently, use this criterion as a complement for the selection of the final water nozzle. In fact, it was possible to measure at the same time the water distribution at the front surface of the fabric and the water mass which falls into the water basin. With the aim to study the influence of the exterior conditions on the final results, it was made two series of tests: one at the inside of the laboratory and other at the outside. In Figure 3.6 and Figure 3.7 it is shown the experimental apparatus at the beginning of the tests

Figure 3.6 - Inside experimental setup for 1st phase tests.

Figure 3.7 – Outside experimental setup for 1st phase tests.

In Figure 3.8 it is shown the performance of the nozzle CW_02 during the 1st phase tests.

Figure 3.8 – CW_02 during 1st Phase tests.

3.3.1. Results

The results obtained in this phase are presented in Table 3.2 and Table 3.3.

Nozzle	Type	$m_{sp.}$ [kg/min]	$m_{col.}$ [kg/min]		$m_{col.}$ [kg/min]	
			Inside	Outside	Inside	Outside
CW_01	Spray curtain	0.87	0.67	0.55	0.20	0.32
CW_02	Spray curtain	1.71	1.22	0.69	0.49	1.02
AT_01	Atomizer	0.16	0.10	0.00	0.06	0.16
AT_02	Atomizer	0.20	0.12	0.01	0.08	0.19

Table 3.2 – Measured values in tests without fire (1st Phase) at 3 bar.

Nozzle	Pressure [bar]	$m_{sp.}$ [kg/min]	$m_{col.}$ [kg/min]		$m_{col.}$ [kg/min]	
			Inside	Outside	Inside	Outside
CW_02	2	1.35	0.83	-	0.52	-
	3	1.71	1.22	0.69	0.49	1.02
	4	2.04	1.14	-	0.90	-

Table 3.3 - Measured values in tests without fire (1st Phase) for CW_02 at 2, 3 and 4 bar.

In Figure 3.10 to Figure 3.16 it is shown the IR results at the end of each test as well as the corresponding photo edited image (using a photo editor software).

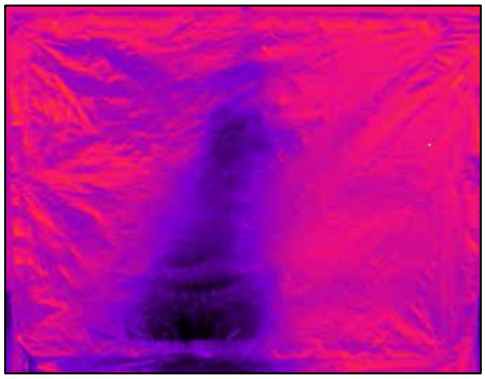

Figure 3.10 - IR image at the end of AT_01 test.

Figure 3.9 - Black and white image of AT_02 tests. Percentage of black: 15.9%

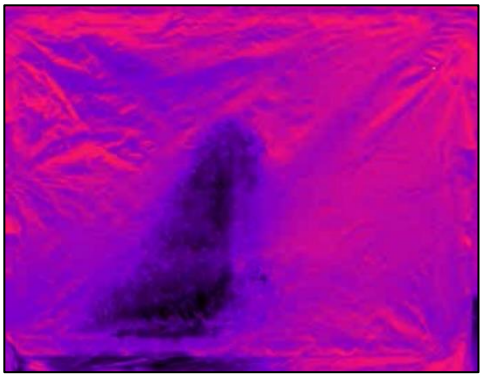

Figure 3.11 -- IR image at the end of AT_02 test.

Figure 3.12 - Black and white image of AT_02 tests. Percentage of black: 14.6%

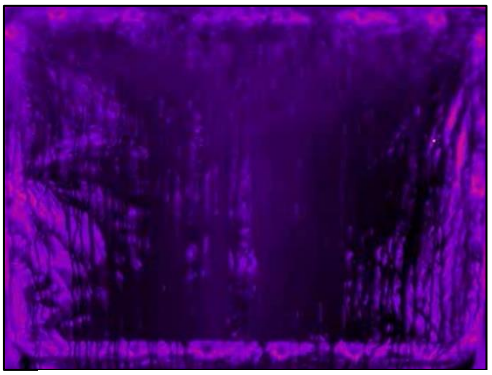

Figure 3.14 - - IR image at the end of CW_01 tests.

Figure 3.13 - Black and white image of CW_01 tests. Percentage of black: 88.5%

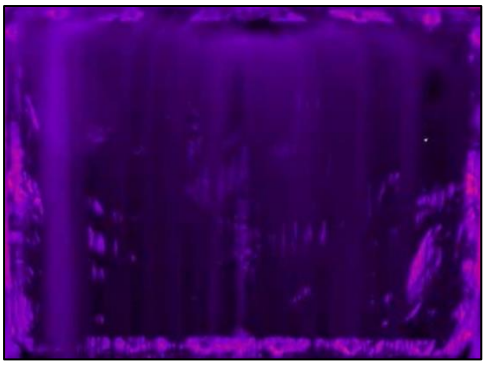

Figure 3.15 - IR image at the end of CW_02 tests.

Figure 3.16 - Black and white image of CW_02 tests. Percentage of black: 95.1%

3.3.2. Discussion

By examining the values presented in Table 3.2, one can conclude that the CW_02 nozzle is the model which has the highest water mass flow rate available. The difference between the values obtained for the inside and outside tests can be justified by the presence of wind. In fact, considering the unpredictable wind characteristics (namely its intensity and direction) and the relatively low water mass flow rates considered, the difference between the results were coherent to the expectations.

The relatively high consumption of water of the spray type nozzle is considered as a disadvantage. As one of the criteria to select the most effective nozzle is the protection of the aluminium layer of the fabric using the minor consumption of water as possible, one can conclude that the atomizer type nozzle are better in this characteristic.

However, through the analysis of the IR camera measurements, it can be visible that the area affected by the falling water for the water spray type is higher when compared to the water atomizer type nozzle.

Due to the relatively high temperature outside the laboratory, the contrast between the wet and dry surface of the fabric is not well observed in the IR recordings. In this way, it was only considered the IR recordings for the interior conditions.

Given the results of this first stage, one can already conclude that the atomizer type water nozzles are not suitable for protection of the fabric in exterior conditions, for two main reasons:

- Presence of wind: considering the very low water mass flow rates used, the wind factor can greatly influence the water coverage area and consequently reduce drastically the cooling efficiency.
- Very reduced water coverage area: Considering the tests inside the laboratory, one can conclude that the area covered by the atomizer type nozzles is lower when compared to spray type ones

Comparing also the ratio between the wetted area and the total front area, it can be seen that the value corresponding to the spray nozzle type is greater when compared to the mist types. In this way, it was chosen the spray type nozzles as the most efficient. The tests described in the 2nd phase will determine which model of the spray type nozzle is more efficient. Despite the atomizer type nozzle been already discarded for the final solution, it was decided to test the atomizer type water nozzles with fire as well.

3.4. 2nd Phase: Tests with fire and airflow

In this phase, fire was used through the burning of a steel basket containing 5kg of forest material (shrubs and eucalyptus leaves). The goal was to simulate a real fire front. Two series of tests were made: one without airflow and another with airflow. Taking advantage of the wind tunnel installed on the facilities in LEIF, the airflow velocity used was 3 m/s. Due to the high distance between the ventilators and the steel basket, the value measured for the airflow speed near the steel basket was 2 m/s. To measure the airflow speed, it was used a *KIMO AMI 300 Hot Wire* sensor. Since the airflow produced by the ventilators has some fluctuations, the value of 2m/s was calculated through an average of the values obtained in the digital anemometer for a period of time of 1 minute.

In Figure 3.17 it is shown the equipment used to evaluate the airflow speed from the ventilators.

Figure 3.17 – KIMO AMI 300 Hot Wire measurements at the beginning of the tests.

One of the aims of this sequence of tests was not only to compare the results involving these two scenarios (namely the fire intensity and temperatures reached at the surface of the barrier) but also be able to analyse the performance of each type of water nozzle when the system is running under different airflow conditions. Through this, one can validate the results in a scenario which is closer to a real fire front

For the tests without airflow, the main conclusion was, even with a minor distance between the fabric and the fuel basket (around 33 cm), the fire intensity was not enough to cause a significant temperature rise in the surface of the barrier. Analysing the IR images, the back surface of the fabric reached a maximum temperature around 70ºC. In fact, when the airflow speed is insignificant, the flames develop mainly in the vertical direction, thus not contacting the fabric. The heat propagation to the barrier is mostly through radiative heat flux, which is not enough to cause visible damage to the fabric. Given this, one can conclude that to achieve better results and to cause the fabric degradation, one had to use airflow to force the contact between the flames and the fabric, increasing the total heat flux to the fabric. Since the tests without airflow did not achieve the expected results, they were discarded.

In Figure 3.18 is shown a schematic representation of the experimental setup used in the 2nd phase tests.

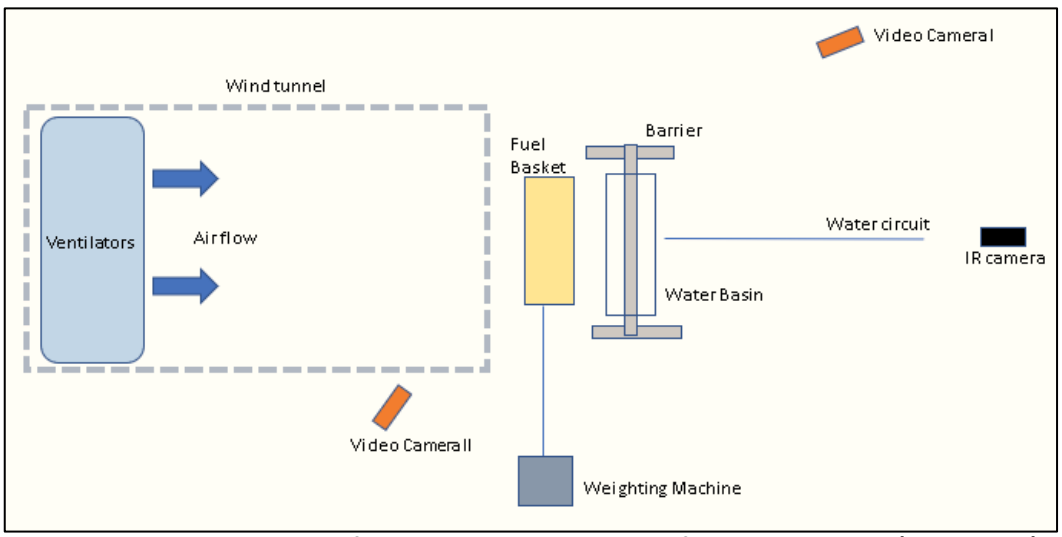

Figure 3.18 - Schematic view of the experimental apparatus for 2nd Phase tests (not in scale).

Two sets of tests were conducted, being the main differences the type of fuel used (shrubs or eucalyptus leaves), the water pressure and type of water nozzle tested.

Since in all the tests inserted in this phase it was used simultaneously fire, airflow and water, they were substantially more complex to manage than the previous phase. All the conditions and methodology adopted were carefully prepared. In Table 3.4 are shown the predefined variables and the corresponding values used in the experiments. All the pre-defined parameters were kept constant during all the tests inserted in this phase in order to ensure that the conditions for each nozzle were the same. Both critical and safe temperature described in Table 3.4 are applied to the fabric.

Nomenclature	Description	Value	Units
$P_{max.}$	Water pump working pressure	3	bar
$T_{crit.}$	Critical temperature	888	ºC
T_{∞}	Safe temperature	150	ºC
Δt	Duration time	140	s
FML	Fuel mass load	5	kg
Fuel	Shrubs Eucalyptus leaves	-	-
V	Airflow speed	2	m/s
$D_{ff.}$	Distance between the fabric and the fuel	33	cm
D_{nf}	Distance between the nozzle and the fabric	24	cm

Table 3.4 – List of the pre-defined parameters used in the 2nd Phase tests.

Some of the parameters described in Table 3.4 will strongly affect the final results. In fact, the value of the water mass flow rate sprayed and the opening angle of each water nozzle, are a function of the working pressure chosen for the experimental tests.

The definition of critical temperature can lead to several interpretations. In the present research study, it is defined as the temperature at which one can observe the fibreglass fabric layer degradation due to the heat, thus being considered the maximum temperature that the fabric can withstand which is 888ºC (according to Batista (2018) experiments).

For the safe temperature, is was defined as the temperature measured at the front of the fabric which corresponds to a temperature of the backside of 50 ºC. As can be seen in Batista (2018), this value is, approximately 150ºC. This set of experiments were conducted with the purpose to select the most effective water spray nozzle by maintaining temperatures closer to the safe temperature threshold throughout the whole fabric for the most amount of time possible.

For each experiment, it was measured:

1. Temperature distribution on the barrier (for both front and back surfaces) as a function of time;
2. Temperature reached by the flames and its evolution with time;
3. Total mass of water which was collected in the water basin;
4. IR temperature profile distribution at the back surface;
5. Fuel burn rate.

Once for this phase it was required the measurements of the temperature evolution at the surface of the barrier, it was used a total of 4 type K thermocouples: one at the backside, two at the front (with one slightly placed to the left side) and one placed at the fuel basket. At the end of each test, it was necessary to replace the fabric with a new one and the thermocouples were maintained at the same location. The nomenclature used to identify each thermocouple is shown in Table 3.5.

For each water nozzle examined in the present study, it was measured the temperatures at all the locations listed in Table 3.5 at an interval of time of 1 second.

Reference	Identification	X-Distance [cm]	Y-Distance [cm]
A0	Middle Front	65	50
A1	Left Front	19	50
A3	Fuel Basket	50	50
A4	Middle Back	68.5	50

Table 3.5 – Reference and respective location of each thermocouple used.

In Figure 3.19 is represented the relative position of the thermocouples as well as the referential used to locate its position.

Figure 3.19 – Referencial used to locate the thermoccouples (back side of the fabric).

As said previously in the present research study, one of the objectives of the experimental tests was to determine the quantity of water that was vaporized. For each nozzle tested, it was measured the total mass of water which was collected in the water basin. The following steps were used to measure these values, and consequently be able to estimate the mass of water which was vaporized:

- At the beginning of the tests, the water basin was placed below the steel frame structure;
- During the tests, the water film fell over the fabric being collected in the water basin.
- At the end of the tests and using a strainer to separate the water of the ashes, it was determined the mass of the water collected.

By determining the mass of the water collected and compare it with the measurements made in the 1st phase, it is possible to estimate the quantity of water that was vaporized during each experiment.

Considering that:

- $Mass\ of\ water\ sprayed = a$
- $Mass\ of\ water\ vaporized = b$
- $Mass\ of\ water\ collected\ in\ the\ water\ basin\ with\ fire = c$
- $Mass\ of\ water\ lost = d$
- $Mass\ of\ water\ collected\ in\ the\ water\ basin\ without\ fire = e$

It follows that:

$$\begin{cases} a = b + c + d \\ d = a - e \end{cases}$$

Consequently, the mass of water which was vaporized is given by:

$$b = e - c$$

Using an IR camera located at the opposite side of exposure and with a certain safe distance to the barrier (Figure 3.20), it can be possible to examine the temperature profile during the tests. This thermal analysis will be made for each test and the final results will be considered as a criterion for the selection of the final water nozzle.

Figure 3.20 – IR camera location in the experiments with fire and airflow tests.

With the aim to obtain the burn rate of the fuel, it was installed a measuring method using a weighing machine. At the beginning of each test, the total mass of the fuel basket (steel structure and fuel) was counterbalanced by an opposite mass. In this way, by resetting the mass measured on the weight machine, it was possible to determine the mass rate loss of the fuel. However, the values given by the balance are not precise as required. In fact, considering that the vertical movement of the steel structure is slightly disturbed by the airflow induced forces, it will affect the final results.

At the end of the tests using shrubs as a fuel, it was made a second series of tests using eucalyptus leaves. In this second series, it was only tested the nozzle CW_02 at different water pressures.

In Figure 3.21 and Figure 3.22 are shown the experimental circumstances during the 2nd phase of tests.

Figure 3.21 – 2nd phase tests using water spray nozzle type and shrubs as fuel.

Figure 3.22 - – 2nd phase tests using nozzle CW_02 and eucalyptus leaves as fuel.

3.4.1. Results

3.4.1.1. Tests using shrubs

In Figure 3.23 to Figure 3.26 are represented the temperature evolution for all the locations considered.

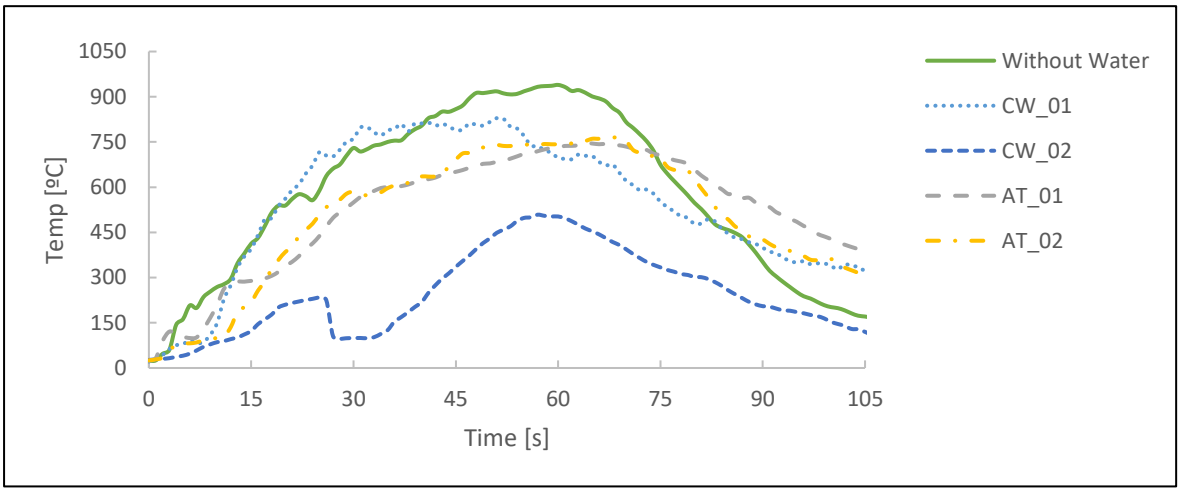

Figure 3.23 – A0 temperature evolution (shrubs).

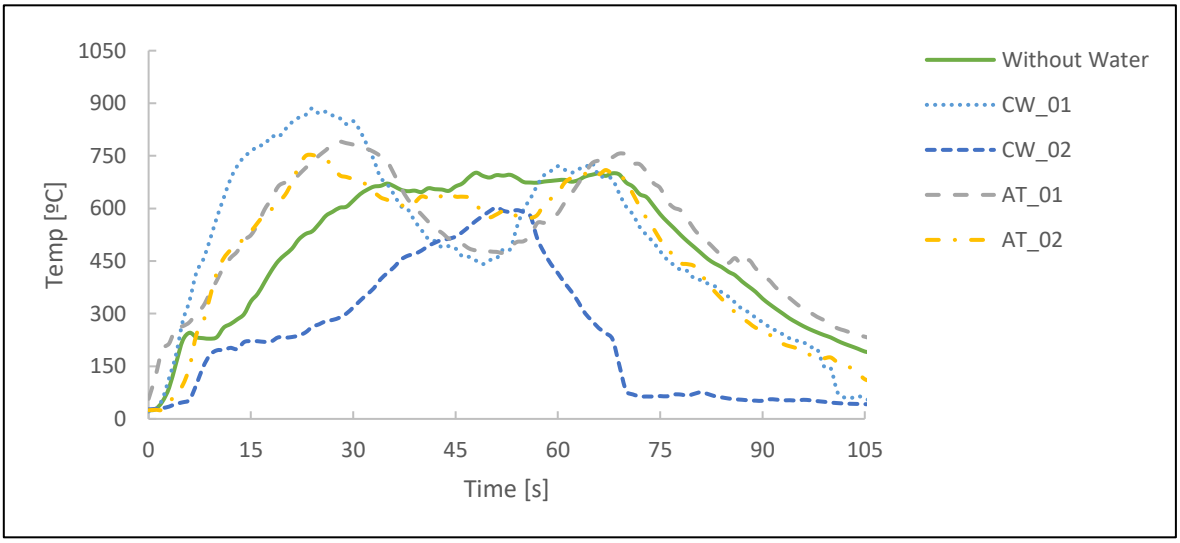

Figure 3.24 – A1 temperature evolution (shrubs).

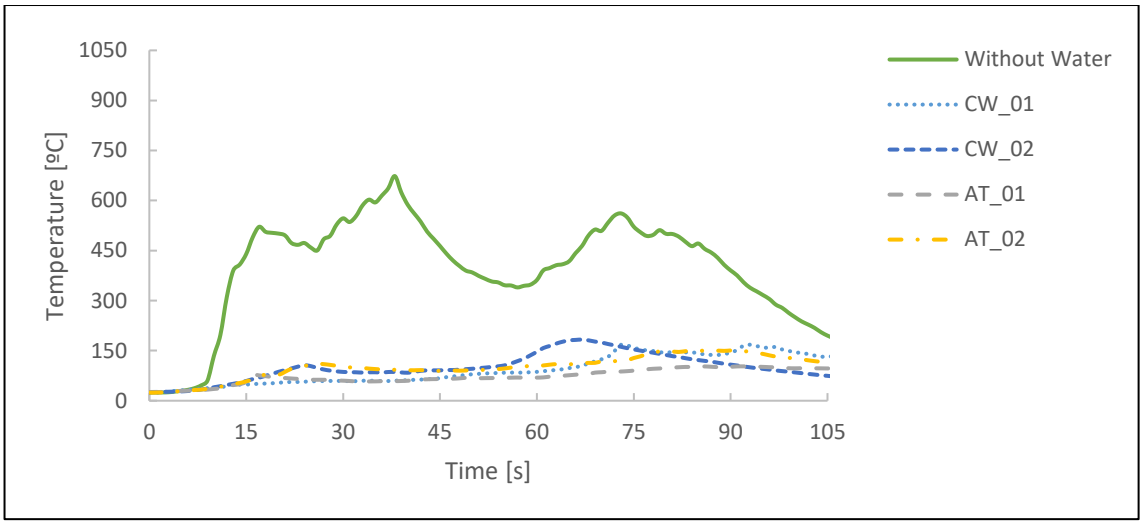

Figure 3.25 – A4 temperature evolution (shrubs).

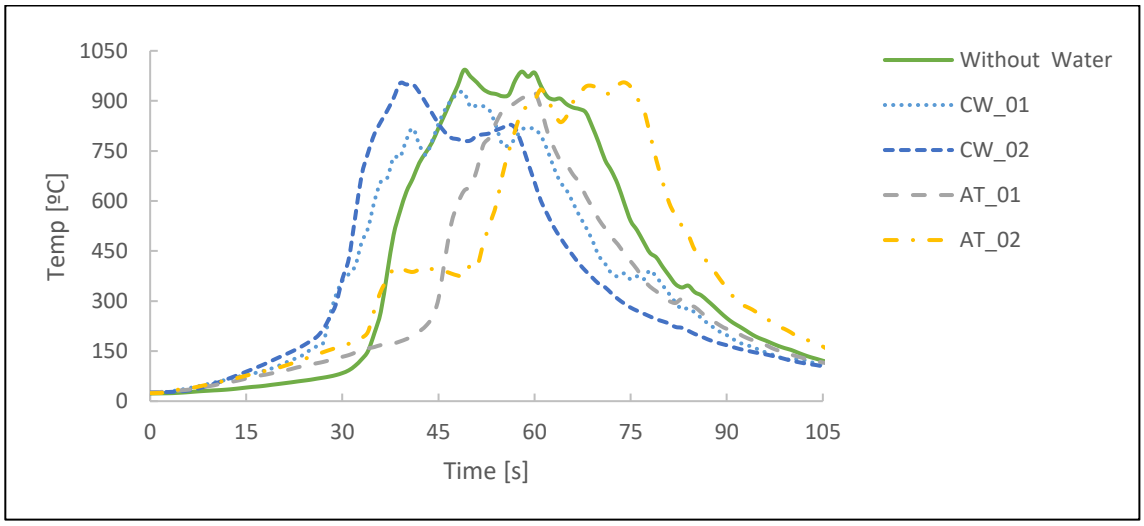

Figure 3.26 - A3 temperature evolution (shrubs).

In Table 3.6 shows the values obtained for the mass of water which was vaporized in each water nozzle test.

Nozzle	$m_{sp.}$ [kg/min]	$m_{col.}$ (1st phase) [kg/min]	$m_{col.}$ (1st phase) [kg/min]	$m_{vap.}$ [kg/min]	WMC_{fuel}
		Inside	Inside	Inside	Inside
CW_01	0.87	0.67	0.22	0.45	14.8
CW_02	1.71	1.22	0.15	1.07	11.5
AT_01	0.16	0.10	0.00	0.10	14.8
AT_02	0.20	0.12	0.00	0.12	14.8

Table 3.6 – Water mass results obtained in 2nd phase tests (using shrubs).

In Figure 3.27 to Figure 3.31 are shown the IR images for each water nozzle tested. All the IR images were taken at the instant of time which corresponds the maximum temperature registered on the steel basket. In this way, the cooling performance of each water nozzle can be compared to each other, since the conditions of exposure were equivalent.

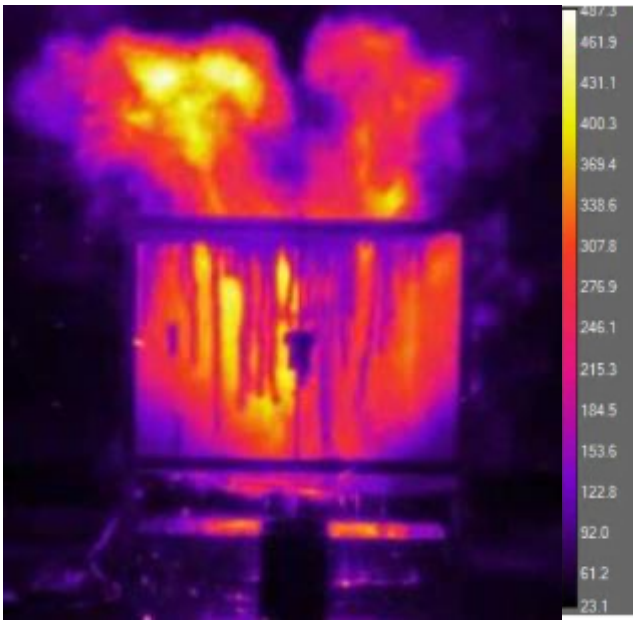

Figure 3.27 – IR image of CW_01 during 2nd Phase tests.

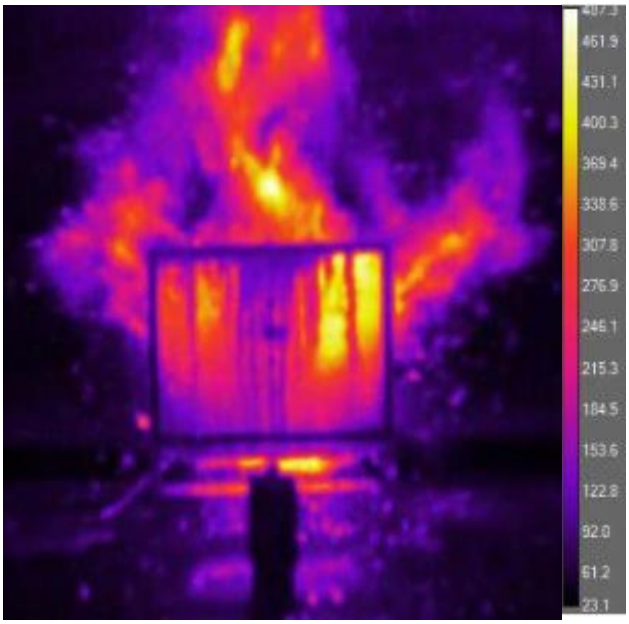

Figure 3.28 – IR image of CW_02 during 2nd Phase tests.

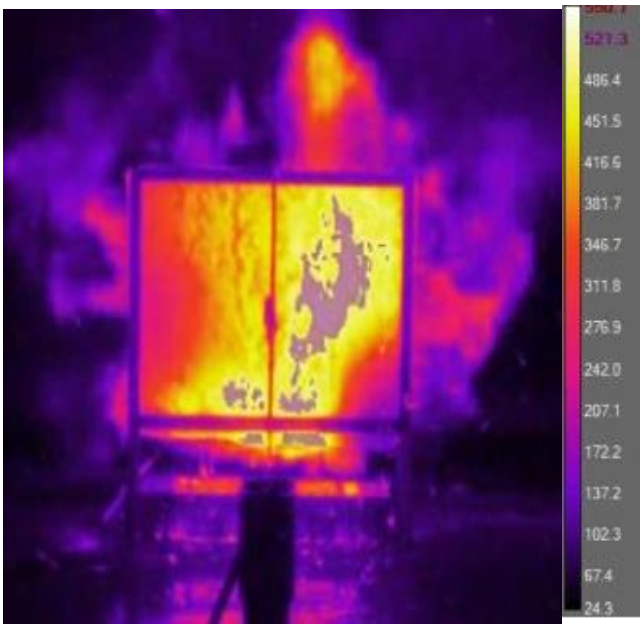

Figure 3.29 – IR image of AT_01 during 2nd Phase tests.

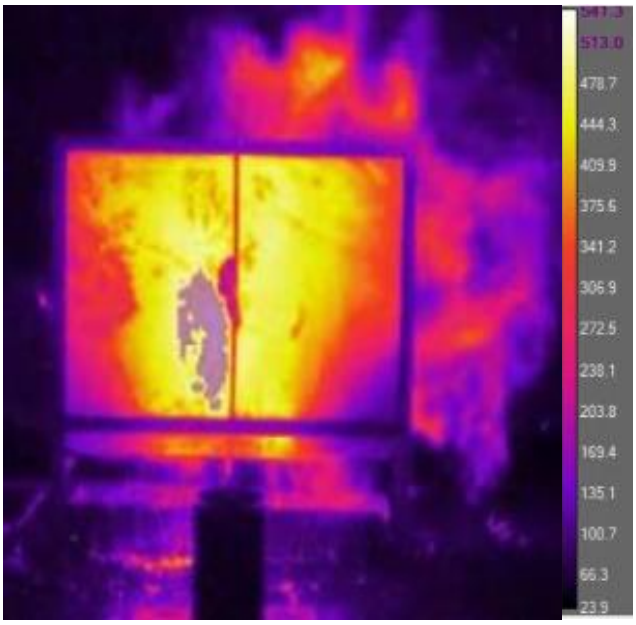

Figure 3.30 – IR image of AT_02 during 2nd Phase tests.

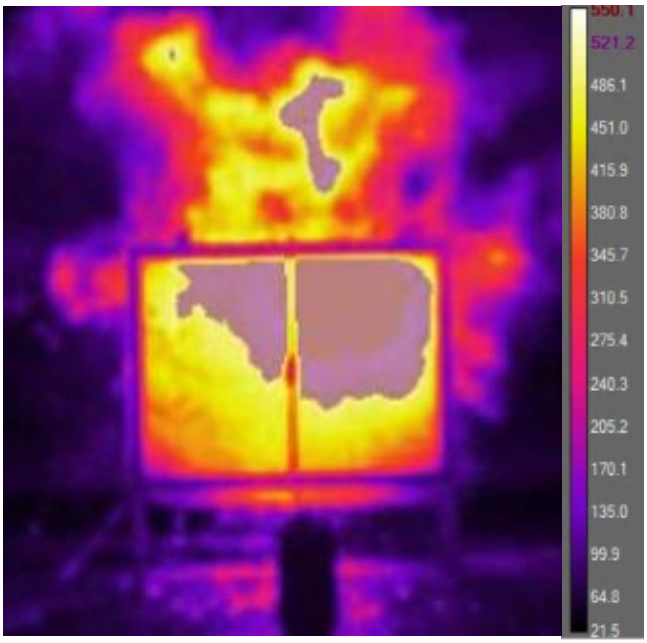

Figure 3.31 –. IR image of 2nd Phase tests without water.

In Figure 3.32 and Figure 3.33 shows the evolution of the steel made basket mass as a function of time and the values for the module of the fuel burn rate, respectively. In both cases, it was used shrubs as fuel. The values were measured at an interval of 10 seconds.

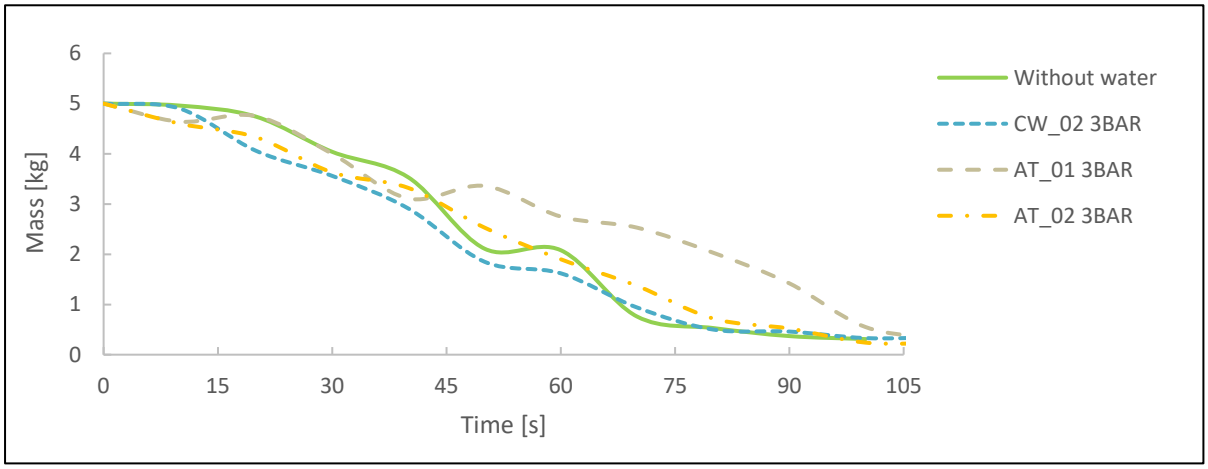

Figure 3.32 -Evolution of the steel basket weight as a function of time.

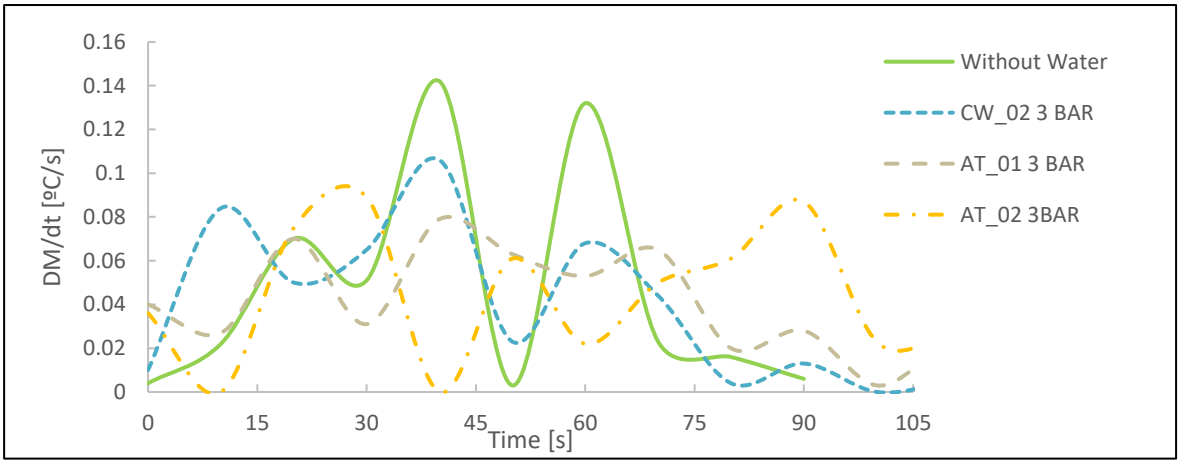

Figure 3.33 – Module of DM/dt values (fuel burn rate) as a function of time.

Due to an acquiring error, it was not possible to measure the values corresponding to CW_01 tests.

3.4.1.2. Tests using eucalyptus leaves

In Figure 3.34 to Figure 3.36 are shown the temperature distribution for the tests using eucalyptus leaves.

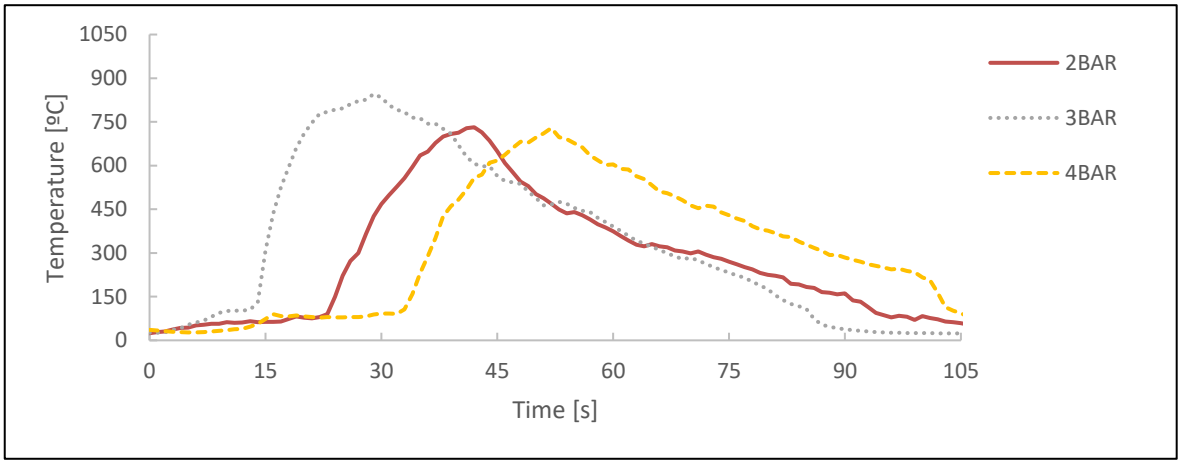

Figure 3.34 - A0 Temperature evolution (eucalyptus leaves).

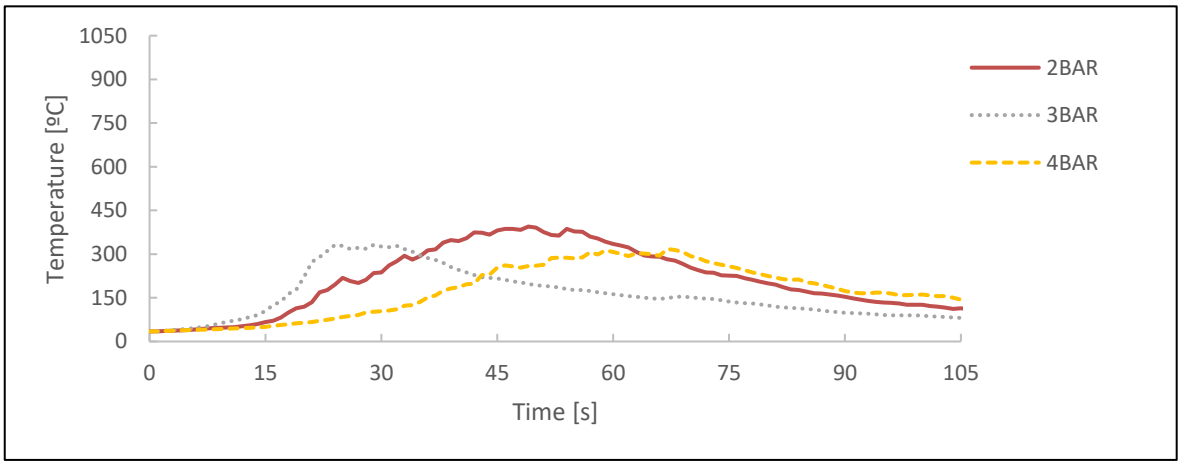

Figure 3.35 – A4 temperature evolution (eucalyptus leaves).

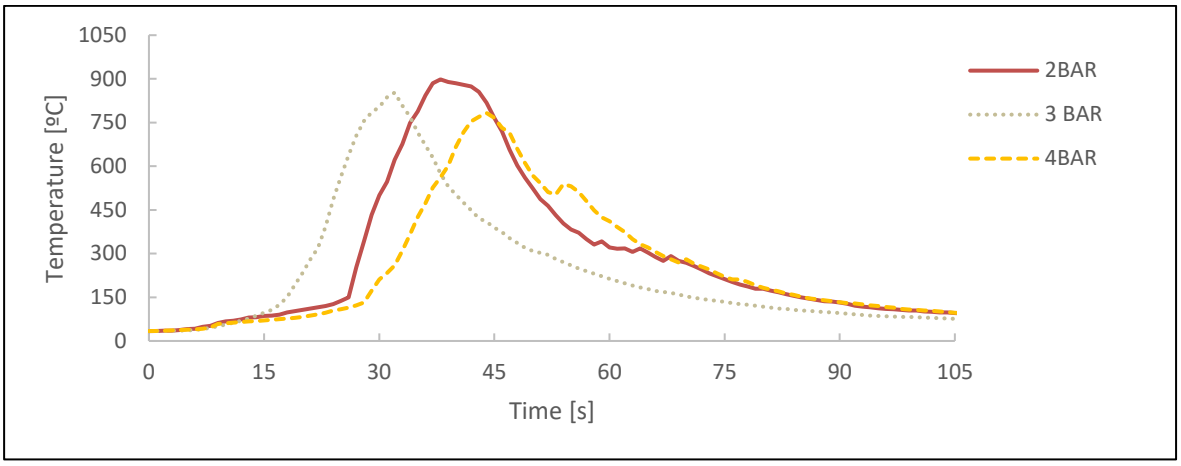

Figure 3.36 – A3 temperature at various water pressures (eucalyptus leaves)

As a result of the malfunction of one thermocouple, it was decided to disregard the temperature measurements at the location left front.

In Table 3.7 shows the values measured for the mass of water which was vaporized at various values of pressure.

Name	Pressure [bar]	$m_{sp.}$ [kg/min]	$m_{col.}$ (1st phase) [kg/min]	$m_{col.}$ (1st phase) [kg/min]	$m_{vap.}$ [kg/min]	WMC_{fuel}
			Inside	Inside	Inside	Inside
CW_02	2	1.35	0.83	0.18	0.65	7.6
	3	1.71	1.22	0.18	1.07	7.6
	4	2.04	1.14	0.35	0.79	7.6

Table 3.7 - Water mass results obtained in 2nd phase tests (using eucalyptus leaves).

Due to the intensity of the fire front is was not possible to obtain satisfactory results for the IR images for the tests using eucalyptus leaves. In this way, these images were discarded.

In Figure 3.37 and Figure 3.38 are shown the evolution of the steel basket mass as a function of time and the corresponding values for the module of fuel burn rate, respectively. In both cases, it was used eucalyptus leaves as fuel.

The values were measured at an interval of 10 seconds

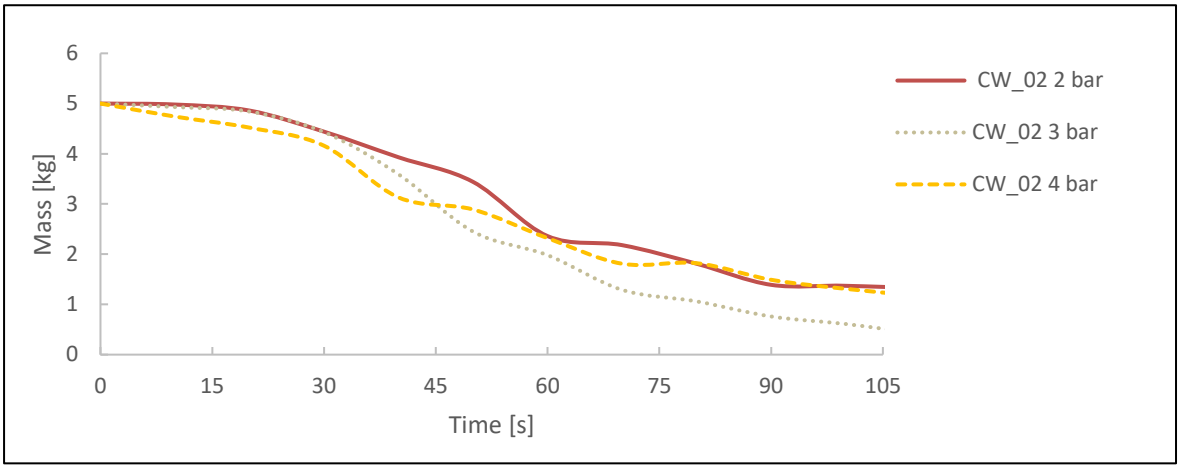

Figure 3.37 - Evolution of the steel basket weight as a function of time

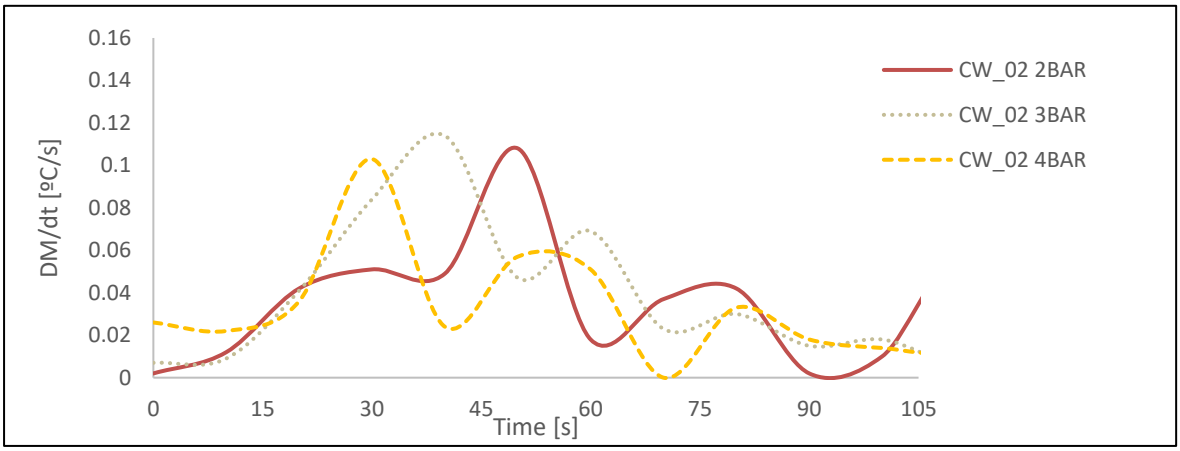

Figure 3.38 - Module of DM/dt values (fuel burn rate) as a function of time.

3.4.2. Discussion

Despite the two types of water nozzles investigated in this study having a significant difference in the values of water mass flow rate sprayed, the analysis of the temperature evolution shows that the influence of the water mass flow rate sprayed is not so important as it was initially expected. For instance, by analysing Figure 3.23 one can conclude that the local surface temperature peak in the AT_01 experiments is lower than the local temperature peak using the nozzle CW_01, despite having a water mass flow rate five times inferior.

Considering only the performance between the two spray type nozzles, in Figure 3.23 one can conclude that the spray nozzle CW_02 has a significantly reduced temperature profile when compared to the results of CW_01. In Figure 3.23, it can be also observed that the behaviour between the two atomizer nozzle models can be considered as equivalent.

By analysing the data showed in Figure 3.34 it can be seen a completely unexpected behaviour. The results obtained shows that the local temperature rise profile using certain models of nozzles (namely CW_01) are higher than the situation where no water-cooling system was activated. These values could be justified by the occurrence of an acquiring error of the thermocouple during the experiment using CW_01 nozzle. Since there is no certainty about the real reason behind this behaviour, it had to be done more tests in order to achieve sustained conclusions.

For each water nozzle tested, there is a high difference between the temperatures peak at the front side when compared to the temperatures measured at the backside. In Figure 3.25, it can be observed the significant influence of the presence of a water film cooling system (regardless of the nozzle type) on the back surface of the fabric. In fact, considering the nozzle with the minimal water mass flow rate measured (0.16 kg/min. for AT_01 nozzle), it was demonstrated that it can be possible to ensure that the back-side temperature of the fabric does not reach values higher than 104ºC using this particular type of water nozzle. Once again, the existence of more tests would be determinant to achieve more sustained conclusions.

As can be seen in Figure 3.26, the fuel basket temperature evolution can be considered as independent of the water nozzle tested. In fact, taking into account that the combustion conditions were practically kept constant during the several tests (with only some differences in the water moisture content of the fuel and the ambient temperature variations), the stable behaviour of the fire trough the several tests confirmed the expectations. Figure 3.26 also demonstrates that the fire intensity evolution was kept constant for all the experiments.

The results obtained can be justified by the fact that these temperatures were obtained from the thermocouples, which could be placed in an area which was receiving more water. In fact, one could see from the previous set of tests (1st phase) that the atomizer nozzles tend to concentrate the water on a small area of the barrier, while the spray nozzles are more efficient at spreading the water through all the fabric area. An analysis of the IR

images corroborates this conclusion, as one can be seen that the high-temperature area of the fabric is much inferior in the spray water nozzles than in the atomizer ones.

In Table 3.6 is shown the confirmation that the atomizer types nozzles are not suitable for the final solution. In fact, for the two atomizer type nozzles tested, the mass of water which was vaporized was equal to the total mass of water sprayed. Consequently, it was not possible to ensure a full coverage area of the fabric with the water film which leads to minor cooling performance.

In fact, considering also the IR measurements, it was possible to evaluate the real cooling difference between the spray and atomizer type nozzle. The dissimilarity between the spray type nozzles (Figure 3.27 and Figure 3.28) and the atomizer type nozzles (Figure 3.29 and Figure 3.30) behaviour leads to the conclusion that for the spray type it is clear the influence of the water film on cooling the fabric as well as on the temperature profile distribution. Considering the IR results for the atomizer type nozzle, one can conclude that the cooling influence is so irrelevant that could be compared to the test without any water system activated (Figure 3.31).

Considering Figure 3.32, it can be seen that the loss of fuel mass per unit of time is almost independent of the water nozzle which is coherent with the expectations.

Regarding the cooling effect on the front surface of the fabric during each test, it can be concluded that the performance of the spray nozzle type is higher than the atomizer type. Taking into consideration Figure 3.23 and Figure 3.24, the selection of the spray nozzle type CW_02 as the finest is well supported since the temperature evolution (as well as the peak value) is lower than CW_01.

To experiment with different kinds of forest fuel, which have in turn different burn characteristics and heat release properties, the last series of experimental tests were made using eucalyptus leaves as fuel. The fuel alteration (with the respective values for calorific power, water moisture content and combustion properties) led to the conclusion that the intensity of the fire was different than the one achieved with the shrub fuel. In fact, comparing the temperature rising between the tests using shrubs and eucalyptus leaves, it is notorious that the eucalyptus leaves have a higher increasing rate.

Considering the fire tests using eucalyptus leaves instead of shrubs, the conclusions regarding the influence of the water pressure (and consequently the water mass flow rate) in the final results were not so obvious. By analysing Figure 3.34, it can be

concluded that, for the same water nozzle, the influence of the water pressure is almost insignificant. In fact, the maximum temperature difference between the test using the maximum pressure of 4 bar and the minimum pressure of 2 bar is only 3ºC. Once again, increasing the number of experiments could help shed some light on this.

Taking a closer look at Figure 3.34, it also shows that the temperature profile obtained for the pressure of 3 bar is higher when compared to the test using a pressure of 4 bar. Considering the values of the water mass flow rate sprayed for these two different pressures (1.35 kg/min. for 3 bar against 2.04 kg/min. for 4 bar) the results were unexpected. This behaviour could be justified by considering that the nozzle itself has different water distribution efficiencies when working at different pressures.

In the measurements of the temperature evolution at the backside of the fabric, the influence of the water pressure is more pertinent. In fact, the values obtained were coherent with the expectations, having a lower temperature profile for the test regarding the maximum water pressure (Figure 3.35).

In Figure 3.36, it can be seen that the fire intensity behaviour using eucalyptus leaves is clearly dissimilar when compared to the temperature evolution using shrubs fuel. These results could be justified by the burning properties of each fuel. Considering that the WMC calculated for eucalyptus leaves is lower when compared to the minimal WMC obtained for the shrubs (7.6 % against11.5%), and also take into account that the difference between their values of calorific power is irrelevant (20 MJ/kg and 22.5 MJ/kg for eucalyptus leaves and shrubs, respectively), it could be considered as a justification for this behaviour.

Comparing Figure 3.33 and Figure 3.38, it can be concluded that the fuel burn rate difference between the shrubs fuel and the eucalyptus leaves is not so dissimilar as it was initially expected. In fact, during the tests, it was possible to observe that the fire intensity using eucalyptus leaves was slightly higher when compared to shrubs. However, the results obtained for the fuel burn rate does not explain the observations. More tests are required to understand this behaviour.

Once the main goal of the cooling system studied in the present thesis is to promote the protection of the fabric in order to ensure peoples and goods safety, it is imperative not only to consider the temperature at the backside of the fabric but also to evaluate the fabric condition after each test. The images of fabric at the end of each test can be consulted in APPENDIX A

Taking into account this criterion, the final selection of the most efficient water nozzle and the corresponding pressure is CW_02 working at a pressure of 2 bar. Despite the results obtained for water pressure of 4 bar been also acceptable, the value of the water mass flow rate sprayed for this pressure is more than 1.5 times higher than the pressure of 2 bar. Considering the objective of protection of the fabric during the longest period of time as possible using the minimal consumption of water as possible, and once the condition of the fabric is equivalent between these two values, the selection of the final pressure of 2 bar is clear.

4. THEORETICAL MODEL VS EXPERIMENTAL RESULTS

As said previously, one of the objectives of this research study was the development of a theoretical modelling in order to understand the complex phenomena related to fire suppression through physical equations. In this way, a comparison between the model predictions and the experimental results has to be made. Due to the model assumptions and resource limitations, it was only possible to compare the results for a reduced number of variables. For this comparison, it was only considered the results obtained for the spray type nozzles since only this type is suitable for the appliance of the theoretical equations. In fact, only this specific type of nozzle was capable of creating a water film which fell over the surface of the fabric.

The results are shown in Figure 4.1 to Figure 4.5. Only the measurements using the front middle thermocouple were considered. To compare the theoretical predictions and the experimental results for the same exposure conditions, in the model it was only considered the water mass flow rate corresponding to each water nozzle or pressure measured in the experiments. In addition, the experimental values obtained for DT/dt corresponds to the time at which the thermocouple reaches each temperature analysed in the model (200ºC to 500ºC).

In the theoretical model, it was assumed that the temperature of the fabric was constant and uniform along its surface and the irradiation emitted from the fire (assumed as a blackbody). This fact leads to the conclusion that only the test using eucalyptus leaves as fuel and CW_02 at a pressure of 3 bar, the total heat flux incident of the surface of the fabric predicted in the simulations is closer to the values obtained in the experiments.

Since the influence of the vaporized water was not initially considered in the model, this fact could justify the difference between the experiments and the model predictions.

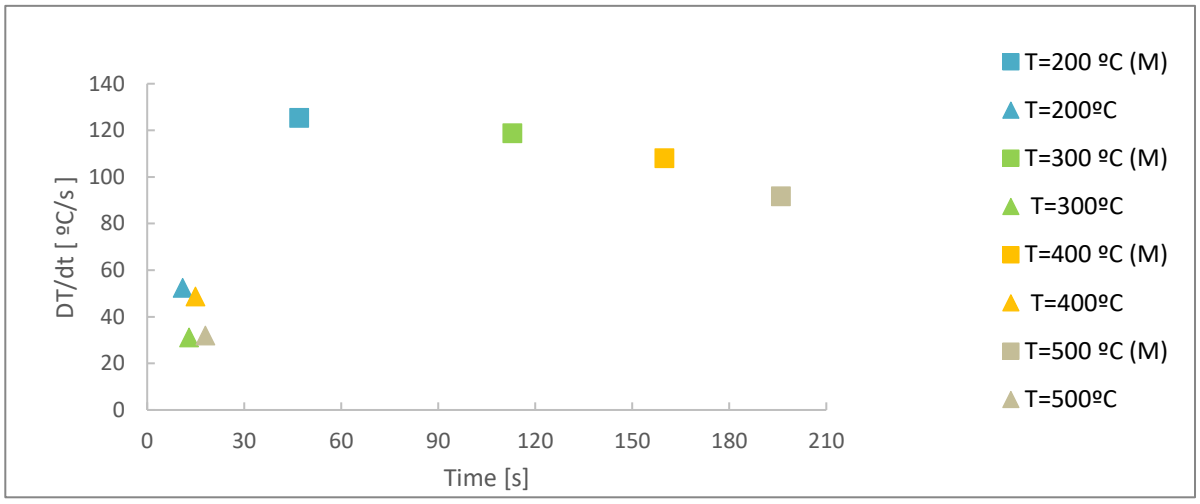

Figure 4.1 - Modelling (M) and experimental results of the nozzle CW_01.

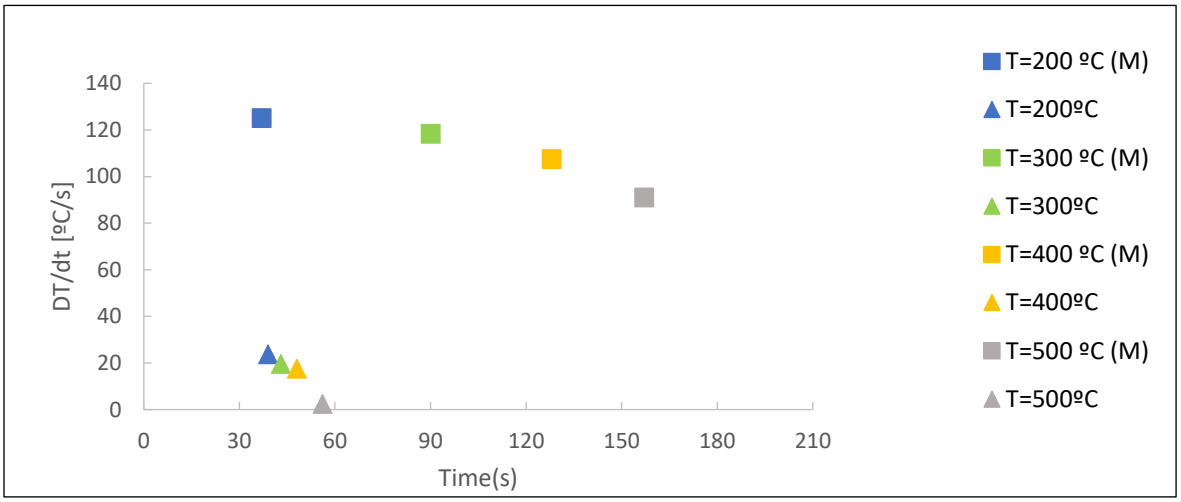

Figure 4.2 Modelling (M) and experimental results of the nozzle CW_02.

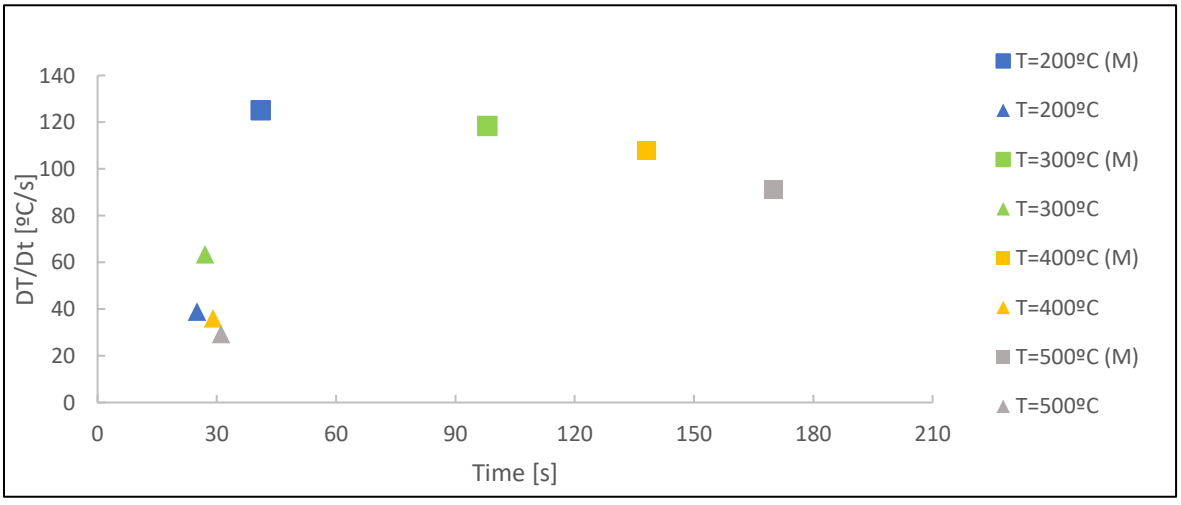

Figure 4.3 Modelling (M) and experimental results of the nozzle CW_02 at a pressure of 3 bar.

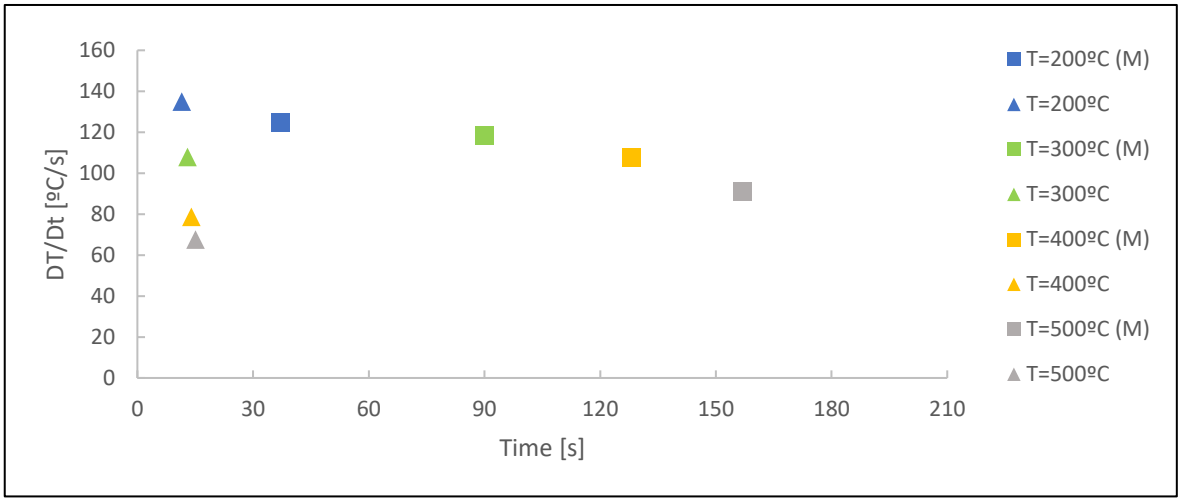

Figure 4.4 - Modelling (M) and experimental results of the nozzle CW_02 at a pressure of 3 bar.

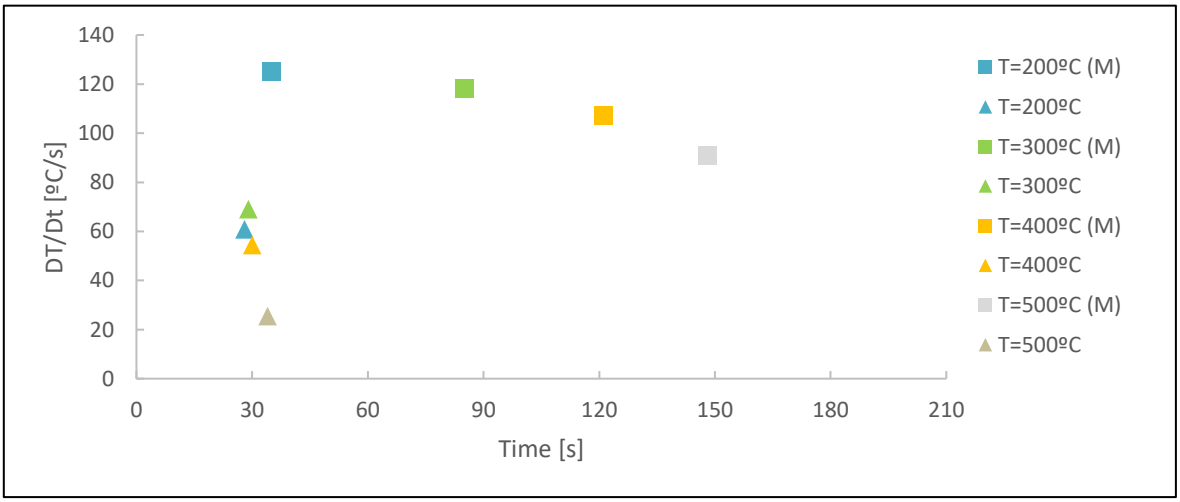

Figure 4.5 Modelling (M) and experimental results of the nozzle CW_02 at a pressure of 4 bar.

However, using the values obtained for the mass of water which was vaporized in the 2nd phase tests, these values can now be inserted in the model and thus be able to improve its predictions. In Figure 4.6 it is shown the comparison between the model predicted values considering the vaporization of water and the model considering vaporization of water (improved version)

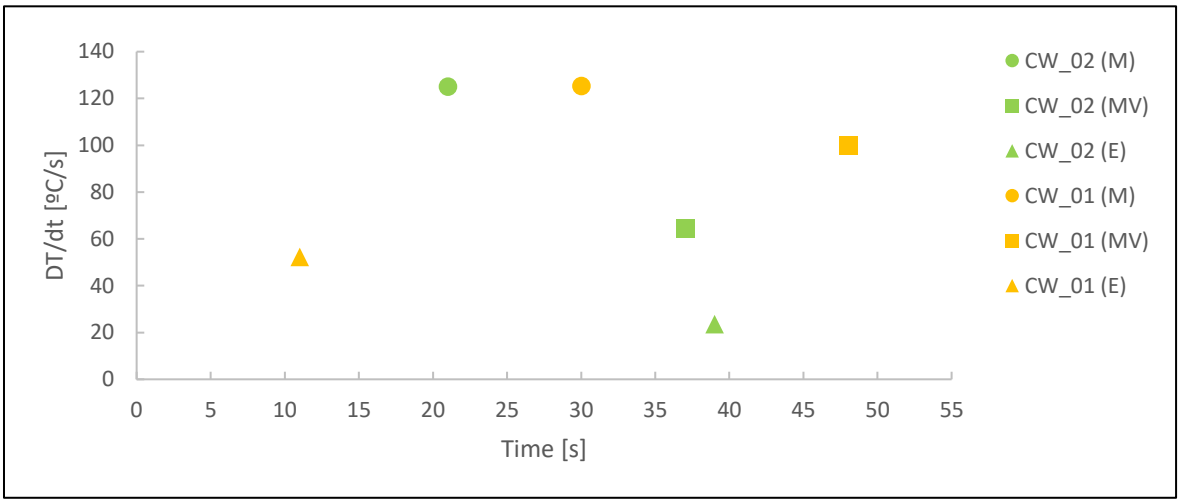

Figure 4.6 - Modelling (M), modelling considering vaporization (MV) and experimental (E) results of the nozzle CW_02 at a pressure of 3 bar.

By analysing Figure 4.6 it can be concluded that the vaporization of the water has a significant influence on the simulated DT/dt values. This fact is coherent with the expectations. In fact, considering value for Hvap. of 2442 kJ/kg (for a temperature of water of 25ºC), the total energy absorbed to cause its vaporization will not be incident in the fabric and consequently the net radiative power at the surface of the fabric is lower. Although the existence of some differences between the experimental results and the improved model predictions, it can be seen that the model could estimate the results with more precision when compared to the initial model version.

Despite the theoretical modelling and the experimental results have different results, in both cases, it was not possible to accomplish a relevant cooling of the fabric (which would result in negative values for DT/dt). Nevertheless, in the experimental results it can be concluded that the presence of a water spray nozzle has the capacity to retard the temperature rise of the fabric.

5. CONCLUSIONS

5.1. Accomplishments

Considering that the destruction and devastation due to wildfires are increasing year after year, the conception of a physical fireproof barrier which can delay the progression of a fire front must be considered one of the most important priorities.

By analysing all the investigations regarding the study of fire suppression using water realized so far, it can be concluded that the present research study is considered as an improvement of the scientific knowledge in this area. In fact, the creation and the study of a fire protection barrier regarding simultaneously a fireproof fabric and a water sprinkler system has never been done so far. In this way, the results achieved in the present thesis could be used in further investigations not only to facilitate the understanding of the complex phenomena behind fire suppression conditions but also to promote the implementation of such devices in the WUI.

For all the experiments, it was only tested one type of fireproof fabric. A total of four different water nozzles (with distinctive values for water mass flow rate available) were tested to achieve the most efficient. Factors such as the condition of the barrier at the end of the fire tests, the total water area coverage corresponding to each nozzle, the variability due to external conditions (namely wind) and the temperature distribution profile were identified for this selection.

It was possible to observe that for a certain type of water nozzle, the exterior conditions has an enormous influence on the water area coverage of the fabric (and consequently in the cooling efficiency). In this way, the application of this type of nozzles in the final solution was immediately discarded.

The effect of the selected water nozzle on the cooling efficiency of the fabric allowed not only to a significant decrease of the temperature profile distribution but also to maintain the fabric fireproof characteristics during a much longer period of time.

By analysing also the IR images during the fire tests it can be confirmed that one particular type of nozzle is much more efficient to promote the cooling of the barrier when compared to the other type. In fact, the IR results show a clear cooling of the fabric as well as a high influence on the temperature rising profile regarding the most efficient type nozzle.

The high complexity associated with the creation of a fire suppression model to predict the behaviour of the system throughout physical equations was considered as an extra motivation to elaborate such analysis. Despite the effort to elaborate such model, by comparing the values predicted in the theoretical modelling to the experimental results, it can be concluded that for the most tests, the heat transfer model does not correspond to the real values with the required precision. However, for a certain experimental test, the difference between the results obtained and the values predicted on the model can be considered as equivalent. This fact leads to the conclusion that, by making some adjustments to the physical equations and the initial assumptions, it can be possible to create such physical interpretation of a fire suppression environment.

During the experimental tests, it was observed some unexpected behaviours. Without having a real justification for some of the results obtained, the realization of more experiments would be determinant to understand such results. Due to time and resource limitations, it was not possible to replicate the experiments. Nevertheless, its description is suggested for further investigations.

Finally, the main objective of conceiving an intelligent fireproof water-cooled barrier which would allow adjusting the total water mass flow rate automatically to properly counterbalanced the total heat flux incident on the fabric was not accomplished. However, a vast number of actions were made in this direction and consequently, the creation of such device is more sustained considering the results obtained in this research study.

5.2. Future Investigations

In spite of the fact of the present research study is a pioneer investigation regarding the protection of fireproof fabrics using a water-cooling system, due to time and resources limitations it was not possible to realize more experiments.

For instance, for the tests with fire and airflow it was required the presence of a minimum of four persons and for each experiment, it was used 5 kg of fuel. In this way, it is enumerated some suggestions to continue this investigation:

- Development of a suitable theoretical model which could represent the scientific phenomenon with more precision;

Despite the predictions given by the theoretical model were equivalent to one of the experimental tests, the initial assumptions do not correspond to reality. For instance, to use the Lumped Capacitance Method, it had to be assumed that the temperature of the fabric is uniform and constant along its entire surface which does not correspond to the observations. However, to justify the application of this method, it was assumed that the temperature of the fabric is uniform and constant, and it is equal to the maximum temperature measured trough the IR images. In this way, it was possible to overcome this difficulty as well as to overestimate the results obtained. The use of the correlation given by Kabov et al. (1995) is not completely suitable for this research study once one of its requirements is that the heat flux incident must be considered constant. This requirement does not correspond to the measurements.

One variable that was not considered in the theoretical modelling was the mass of water which was vaporized during the fire tests. Considering that the vaporization of the water requires the absorption of a great amount of energy, the real energy which was incident in the fabric is minor when compared to the situation when the vaporization of the water does not occur. Consequently, this variable would influence the final predictions of the model.

- Adjustment of the steel structure in order to ensure that the flames do not affect the IR camera recordings;

Since for the fire tests it was used the ventilators to promote the rise of the total heat flux incident on the fabric and thus promoting its destruction, it has associated one disadvantage. According to the observations and the IR measurements, the airflow speed was sufficient to create a fire plume which could englobe all the barrier. In this way, it was

not possible to ensure the precise measuring of the temperature values during this phenomenon. In addition, the intensity of the fire plume regarding the test with eucalyptus leaves was so intense that the fire plume covered the backside of the fabric during the duration of the experiment. To be able to overcome this difficulty, it has to be done some changes to the steel frame. By increasing all the four sides of the steel structure, it is possible to ensure that only the surface of the barrier is measured on the IR camera. In this way, the measurement of the temperatures at the back surface of fabric is always possible to obtain during the time of the experiment.

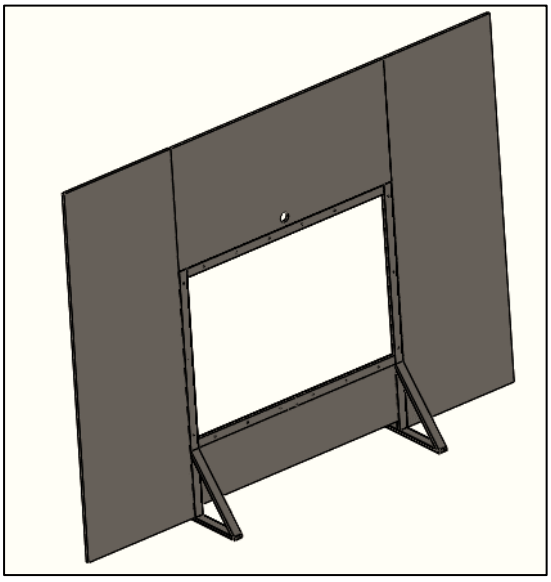

Figure 5.1 - 3D view of the upgraded steel frame.

- Creation of a system which could give the ability to change the distance between the nozzle and the fabric as well as a method to align the nozzle perfectly to the fabric in order to reduce lateral water losses.

One of the difficulties of the tests without fire was to ensure the correct alignment of each water nozzle tested. This factor could influence the values for the mass of water which was considered as lost.

- Development of an automatic software which regulates the amount of water mass flow rate in order to counterbalance the fire radiation

The objective of creating an intelligent water-cooled fireproof barrier was not achieved. However, important steps were made in this direction. It was idealized the following stages to elaborate such a system:

I. Using a fire sensor intensity, be able to evaluate the intensity of the fire at the front surface of the fabric (defined as T_m) at a pre-establish period of time;

II. Throughout physical equations, a software calculates the value of the water mass flow rate required (defined as Q_r) to the temperature of the fabric measured reaches the pre-defined safe temperature.

III. Once calculated this value, it is used as an input to a proportional electric activated valve which adjusts the water mass flow rate according to the calculations (defined as Q_o).

In Figure 5.2 is shown a schematic representation of the steps mentioned above:

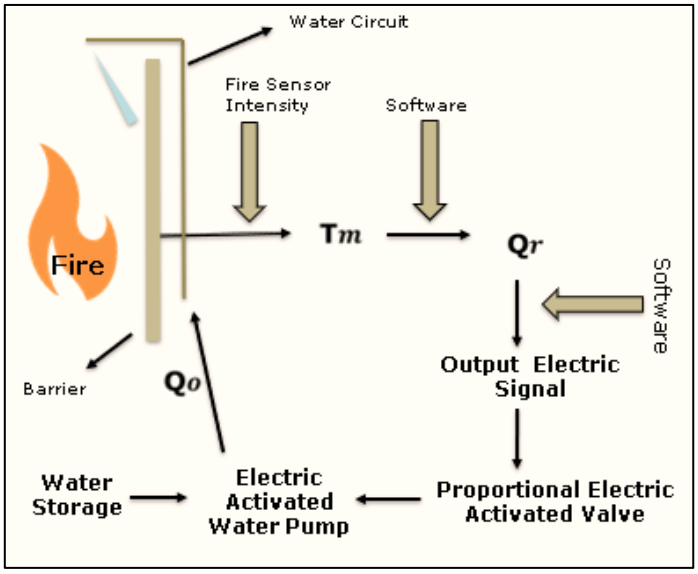

Figure 5.2 – Representation of the required steps to create an intelligent fire-resistant water-cooled barrier.

One of the most suitable proportional electric activated valves to use in this configuration is the 2/2 proportional seat valve produced by "Hauhinco Valves" n.d..

- It was assumed that the value of the water mass lost is the same for the tests with fire and airflow and the ones without.

It would be necessary more experiments to obtain the difference between these two scenarios and consequently be able to estimate, with more precision, the quantity of water which is vaporized during the tests with fire.

- Adjustment of the position of the water nozzle to optimize the quantity of water which falls over the surface of the fabric.

Once the direction of the water sprayed from the spray type nozzle was perpendicular to the vertical surface of the fabric, it resulted in a certain amount of water which, as soon as it reaches the surface, is projected and falls outside the water basin thus considering as lost. Considering a theoretical setup with the difference of the nozzle is positioned with a certain angle to the vertical fabric, it would result in an improvement of the total mass of water which covers the fabric thus minimizing the water which is lost.

By accomplishing the recommendations mentioned, it will result not only in the conception of an efficient system which helps to protect human lives but also represents significant progress of the scientific knowledge in such complex theme as the study of wildfires and the development of protection mechanisms.

BIBLIOGRAPHY

Al-Khalil, K. M., Keith, T. G., & De Witt, K. J. (1991). Hydrodynamic and thermal analysis of rivulet flow down a vertical solid surface. *International Journal of Numerical Methods for Heat & Fluid Flow*, *1*(1), 63–76. https://doi.org/10.1108/eb017474

ASTM, I. (2015). ASTM E2707. Retrieved from https://www.astm.org/Standards/E2707.htm

ASTM, I. (2017a). ASTM E2748. Retrieved from https://www.astm.org/Standards/E2748.htm

ASTM, I. (2017b). ASTM E814 - 13a. Retrieved from https://www.astm.org/Standards/E814.htm

ASTM, I. (2019). ASTM E2307. Retrieved from https://www.astm.org/Standards/E2307.htm

Batista, R. M. (2018). *Mechanisms for Active Protection of People and Infrastructures against Forest Fires*. Coimbra.

Buchlin, J. M. (2005). Thermal shielding by water spray curtain. *Journal of Loss Prevention in the Process Industries*, *18*(4–6), 423–432. https://doi.org/10.1016/j.jlp.2005.06.039

Gelaude, J. (1984). *Automatic Fire Protection System*. https://doi.org/US005485919A

Hauhinco Valves. (n.d.). Retrieved from https://www.hauhinco.de/en/products-services/valves/water-hydraulic-valves-proportional-valves/

Incropera, F., Bergman, T., Lavine, A., & Dewitt, D. (2011). *Fundamentals of Heat and Mass Transfer* (7th ed.).

Kabov, O. A., Diatlov, A. V., & Marchuk, I. . V. (1995). Heat Transfer from a Vertical Heat Source to Falling Liquid Film. *Proceedings of the First International Symposium on Two--Phase Flow Modeling and Experimentation*, *1*, 203–210.

Lev, Y., & Strachan, D. C. (1989). A study of cooling water requirements for the protection of metal surfaces against thermal radiation. *Fire Technology*.

https://doi.org/10.1007/BF01039779

Meredith, K., De Vries, J., Wang, Y., & Xin, Y. (2012). A comprehensive model for simulating the interaction of water with solid surfaces in fire suppression environments. *Proceedings of the Combustion Institute*, *34*(2), 2719–2726. https://doi.org/10.1016/j.proci.2012.06.094

Orrange, T., & Sweeton, G. (2002). *WILDFIRE PROTECTION SYSTEM*.

Pordata. (2018). Total burnt area in Portugal. Retrieved from https://www.pordata.pt/Portugal/Incêndios+rurais+e+área+ardida+–+Continente-1192-310375

RISE Research Institutes of Sweden. (2017). EN 1363-1. Retrieved from https://www.sp.se/en/index/services/firetest_building/fire_constructions/fireresist/generel/Sidor/default.aspx

Smith, T., & Smith, H. (1988). *FireProof Building Panels*. (19).

Soares, D. (2018). *Análise de Acidentes com Viaturas . Sistema de Proteção de Autotanques* .

ANNEX A

The nozzles used in the present research study are produced by Boquillas de Aspersion. The reference used in this thesis to identify each nozzle is the same as the reference used by this company, except for the atomizer type which the reference of AT_01 and AT_02 which corresponds to DF_01 and DF_02, respectively.

In Table 0.1 and Table 0.2 are shown the technical characteristics of each type of water nozzle tested in the present study.

Water mass flow rate [L/min]

Name	0.3 bar	1 bar	2 bar	3 bar	5 bar	ang@3bar
CW_01	0.3	0.7	0.8	1	1.4	170º
CW_02	0.6	1.4	1.8	2.5	3.2	170º

Table 0.1 – Technical characteristics of the spray type nozzles tested.

Water mass flow rate [L/min]

Name	2 bar	5bar	âng@3bar
AT_01	0.11	0.175	70º

Table 0.2 - Technical characteristics of the atomizer type nozzles tested.

It was not possible to obtain the technical information of the water mass flow rate for AT_02 nozzles.

In all the fire tests which were made, it was used the same type of fabric, in Table 0.3 it is represented also its technical data, given by the manufacturer ERICA (TVL126)

Properties	Units	Value
Composition		Textured E fibreglass filaments
Finished		Aluminium foil 1 side
Weight	Gr/m2	520
Thickness	mm	0.4
Fibreglass diameter	micron	6-9
Weave		Satin
Ends-Picks 10cm		
-warp		45
-weft		110
Strength Warp	N/50 mm	3840
Strength Weft	N/50 mm	2240
Service Temperature		
- Short Periods	ºC	550
-Continuous		150

Table 0.3 - Technical characteristics of the model of the fabric tested.

APPENDIX A

In the current appendix, it is shown several IR and real images during each test as well as the fabric condition at the end of each experiment.

Figure 0.1 - Fabric condition before each fire test.

- **Tests using shrubs:**

Figure 0.2 – Nozzle CW_01 at a pressure of 3 bar during 2 minutes of exposure.

Figure 0.3 - Nozzle CW_02 at a pressure of 3 bar during 2 minutes of exposure.

Figure 0.4 - Nozzle AT_01 at a pressure of 3 bar during 2 minutes of exposure.

Figure 0.5 - Nozzle AT_02 at a pressure of 3 bar during 2 minutes of exposure.

Figure 0.6 - Test without any water system during 2 minutes of exposure.

Figure 0.7 - Nozzle CW_02 at a pressure of 2 bar during 2 minutes of exposure.

- **Tests using eucalyptus leaves:**

Figure 0.8 – Nozzle CW_02 at a pressure of 2 bar during 2 minutes of exposure.

Figure 0.9 - Nozzle CW_02 at a pressure of 3 bar during 2 minutes of exposure.

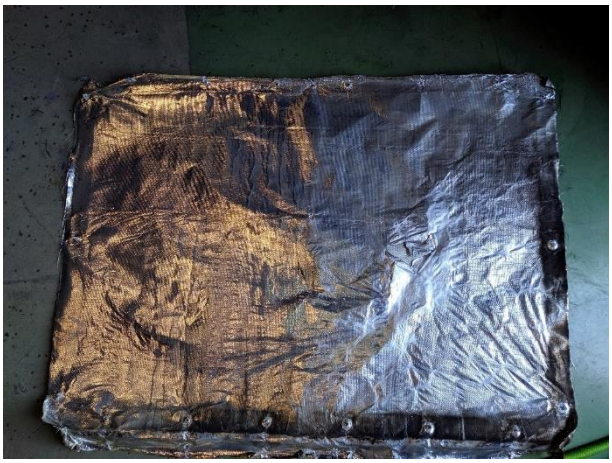

Figure 0.10 - Nozzle CW_02 at a pressure of 4 bar during 2 minutes of exposure.